공학석사학위논문

Cloning and expression of small laccase Sv1 from *Streptomyces viridosporus* and its application to develop dyeing strain for wool fabrics and polyol chain extender for self-healable polyurethane

방선균 유래의 락케이즈 Sv1의 클로닝, 발현을 통한 양모 염색 균주의 개발 및 자가 치유가능 PU 생성을 위한 폴리올 사슬 연장체의 합성

2020년 8월

서울대학교 대학원

화학생물공학부

노 희 원

Cloning and expression of small laccase Sv1 from *Streptomyces viridosporus* and its application to develop dyeing strain for wool fabrics and polyol chain extender for self-healable polyurethane

By

Heewon Nho

Advisor: Professor Byung-Gee Kim, Ph.D.

Submitted in partial fulfillment of the requirement for the Master of Science in engineering degree

August, 2020

School of Chemical and Biological Engineering
Seoul National University

공학석사학위논문

Cloning and expression of small laccase Sv1 from *Streptomyces viridosporus* and its application to develop dyeing strain for wool fabrics and polyol extender for self-healable polyurethane

방선균 유래의 락케이즈 Sv1의 클로닝, 발현을 통한 양모 염색 균주의 개발 및 자가 치유가능 PU 생성을 위한 폴리올 사슬 연장체의 합성

지도교수 김병기

이 논문을 공학석사 학위논문으로 제출함

2020년 7월

서울대학교 대학원

화학생물공학부

노희원

노희원의 공학석사 학위논문을 인준함

2020년 7월

위 원 장 _____ (인)

부위원장 _____ (인)

위 원 _____ (인)

Abstract

Heewon Nho
Chemical and biological engineering
The Graduate School
Seoul National University

Polyurethane (PU) has 6 % of the total global polymer market resulted from versatile applications. The development of biodegradable and sustainable material is essential to solve the serious environmental problem in petrochemical polyol and demand of biological content increase. Aromatic monomers in PU are usually made from petroleum, exerting serious toxicity in human neural system as well as depriving of fossil resources. In this research, we provided byproduct derived from lignin decomposition as aromatic chain extenders, which can replace 1,4-butanediol. Lignocellulos biomass monomer, vanillin-based polyol chain extender gives excellent mechanical properties to the PU elastomer.[1] Herein, we expanded perspectives into developing environmental PU elastomer with self-healing property. We reported enzymatic and chemical synthesis methods of new eugenol based compound, dieugenol-based hexaol. Dieugenol based polyurethane has 6.3 Mpa of tensile strength and 0.016 Mpa of Young's modulus, and -75.6 ℃ of glass transition temperature. Eugenol based polyurethane has reversible urethane bond after heat treatment for 3 hours at 150 ℃, the PU elastomer had the self-healing efficiency of 84.7 %.

Recently, bio-inspired dyeing methods using oxidative enzymes such as laccase, peroxidase have been used to enhance the color depth of fabrics. Here, a novel and eco-friendly dyeing method using recombinant *Streptomyces glaucescens* was investigated, which has a great potential for application in textile processes. Especially, we used both melanin- and laccase-secreting cells instead of purified laccase for applying this system to cost effective industrial-grade biocatalysts for coloration. At first, we evaluated a performance of laccase secretion as well as a dye production in the supernatant of liquid cultures of the transformed cells. Dosages of inductor and induction time were optimized for effective laccase secretion and dye production. Afterwards, cell supernatants containing laccase and melanin were exploited for coloration of wool fabrics. The properties of colored wool fabrics were evaluated in terms of color depth and color fastness. Also, binding of the melanin with wool fabric was verified with Fourier transform infrared spectroscopy, surface morphology, and color fastness test. These results would provide an inspiration in extending research activities on this one-pot cellular system and in replacing isolated enzyme system.

Key Words: laccase, polyol chain extender, self-healable polyurethane elastomer, one-pot coloration, wool fabrics

Student Number: 2018-27445

Contents

CHAPTER Ⅲ

Laccase mediated one-pot dyeing of wool fabrics using recombinant *Streptomyces gluacescens*

List of Figures

Figure S2. HPLC analysis of enzymatic reaction products using recombinant BmOMT and BlOMT enzyme.

Figure S3. ESI-MS/MS patterns for compounds A, C, and D

List of Tables

List of Abbreviations

Eugenol oxide	3-(4-hydroxy-3-methoxyphenyl)propane-1,2-diol
Eugenol oxide dimer	5-3,3'-(6,6'-diepoxy-5,5'-dimethoxy-[1,1'-biphenyl]-3,3'diyl)bis(propane-1,2-diol)
Vanillyl glycol	3-(4-hydroxy-3-methoxyphenyl)propane-1,2-diol
Vanillyl acetonide	4-((2,2-dimethyl-1,3-dioxolan-4-yl)methyl)-2-methoxyphenol
Vanillyl acetonide dimer	5,5'-bis((2,2-dimethyl-1,3-dioxolan-4-yl)methyl)-3,3'-dimethoxy-[1,1'-bisphenyl]-2,2'-diol
Dieugenol-based hexaol	3,3'-(6,6'-dihydroxy-5,5'-dimethoxy-[1,1'-biphenyl]-3,3'diyl)bis(propane-1,2-diol)

Chapter I

Cloning, expression, and purification of a small laccase Sv1 from *Streptomyces viridosporus*

1.1. Introduction

Laccase (EC 1.10.3.2, *p*-diphenol:dioxygen oxidoreductase) belongs to the superfamily of multicopper oxidases and participates in cross-linking of monomers, degradation of polymers, and ring cleavage of aromatic molecules. [1] It has attracted much attention because it can catalyze the one-electron oxidation of substrate molecules and transfers four electrons to reduce O_2 to H_2O. For these reasons, it is widely used in the synthesis of organic molecules, where typical substrates are phenols and amines. [2]

Laccases from white-rot fungi, *Trametes* sp. or *Pleurotus* sp, have been most exhaustively investigated [3] because most of the fungal laccases exhibit high redox potentials and relatively high activities toward substrates [4]. Unfortunately, they are only able to function within a narrow range of acidic pH and mesophilic temperature. Besides, fungal laccases are highly glycosylated enzymes and often fail to be expressed in bacterial systems. Recent studies on metagenomics libraries and evolutionary data [5,6] demonstrate laccases or laccase-like enzymes exist in bacteria. More than 2200 laccases have been classified from available genome sequences and structural data and 1000-2000 potential bacterial laccases have been assigned into 5 different superfamilies.

However, it still remains unknown about the physiological functions of most bacterial laccases. Some functions were reported to be

spore pigmentation in the case for CotA from *B. subtilis* and copper homeostasis in *E. coli* (CueO) and *Corynebacterium glutamicum* (CopO). [7,8,9,10]

Recently, the characteristics and functions of the bacterial enzymes are being investigated but still a few studies on bacterial laccases have been done. The reports have described the thermal robustness and alkaline optimal pH of bacterial laccases compared to fungal enzymes. For example, the laccase from *Thermus thermophilus* shows excellent thermal stability [12], and laccases from *Bacillus halodurans* and *Streptomyces coelicolor* exhibit optimal pH around 7.5 or 9.4. [13,14] This kind of bacterial alkaline laccase may help to overcome the limitations of fungal laccases and extend industrial applications of laccase at higher pH conditions, elevated reaction temperatures, and prolonged operations.

Here, we describe the cloning, expression and characterization of the small two-domain Sv1 laccase from *Streptomyces viridosporus*. Sv1 demonstrated moderate thermostability and neutral activity profile in a wide pH range up to pH 9 and stability in presence of organic solvents. Thereby its catalytic properties were distinct from other laccases.

1.2. Materials and methods

1.2.1. Chemicals and materials

LB Broth were purchased from BD bioscience. 2,2'-Azino-bis(3-ethylbenzthiazoline-6-sulfonic acid) and L-dopa were purchased from Sigma-Aldrich. Oligomers and sequencing were purchased from Bionics (Seoul, South Korea). All commercially available solvents (GR grade) or reagents were used without further purification unless otherwise noted.

1.2.2. Protein expression

All the expression of enzymes was conducted using *E. coli* BL21 (DE3). Each of the constructed vectors was transformed into the competent cell and selected on a LB agar plate supplemented with appropriate antibiotics. Single colony was inoculated into LB broth with the according antibiotic and grown overnight at 37 ℃. 500 μl of the seed culture was inoculated into 50 ml of LB media and grown at 37 ℃ until the cell density reached OD_{600} = 0.6 ~ 0.8. Expression of laccase was induced by addition of 0.1 mM IPTG with further overnight incubation at 18 ℃. The cells were harvested by centrifugation at 3,200 xg for 15 min and washed with PBS buffer solution. The cells were resuspended in Tris buffer solution containing 50mM Tris-HCl pH 8.0, 200mM NaCl, and 10% Glycerol. The

cell soup was disrupted using ultrasonication in ice-chilled water for 5 min (5s on, 72s off). The soluble fraction was collected by centrifugation of the cell lysate at 13,000xg for 30 min at 4 ℃. After denaturation process, the total and soluble fraction of lysates were loaded into SDS-PAGE.

1.2.3. Laccase activity assay

The activity of Sv1 towards the substrates 2,2′-azino-bis(3-ethylbenzothiazoline-6-sulphonic acid (ABTS), guaiacol, and L-dopa was tested in 50 mM sodium citrate buffer (pH 3–6), 50 mM potassium phosphate buffer (pH 7–9) at room temperature. The oxidation of ABTS (0.5 mM) was followed at 420 nm (ε = 36 $mM^{-1}cm^{-1}$), oxidation of guaiacol (2 mM) to the dimeric product tetraguaiacol was followed at 470 nm (ε = 26 $mM^{-1}cm^{-1}$) and oxidation of L-dopa (1 mM) was followed at 525 nm (ε = 65 $mM^{-1}cm^{-1}$). Activity assays were performed in triplicate. For pH activity profiles, activities at optimal pH were set as 100%.

For testing thermal stability, Sv1 (in 50 mM sodium citrate buffer with pH 5.0) was incubated at 20 ℃, 30 ℃, 40 ℃, 50 ℃, 60 ℃, 70 ℃, 80 ℃, 90 ℃, 100 ℃ for 60 min. After incubation, samples were immediately chilled on ice. Residual activities were measured with ABTS as described above. Data were collected as triplicate.

Relative activities of Ssl1 in presence of organic solvents were determined after 10 min incubation in sodium citrate buffer (50 mM, pH 5.0) containing solvent in indicated concentrations at ambient temperature. Activities were measured with ABTS as described above.

1.3. Results

1.3.1. Soluble expression and purification of laccase Sv1

For Sv1 expression, cultures were grown in LB medium at 37° C until OD_{600} reached 0.6 when expression was induced by only 100 μM IPTG with 2 mM copper sulfate as supplement. After harvesting cell, the soluble fraction was applied to His-tag purification step which resulted in homogeneously pure Ssl1 as judged by SDS-PAGE (Fig.1). Sv1 is concentrated 16-fold by ultrafiltration with specific activity of 102 U mg^{-1}.

1.3.2. Optimal conditions for laccase activity

1.3.2.1. Effect of pH

The optimum value of pH varied according to the substrate because different substrate caused different reaction for laccases (Fig.1.2(a)). In all cases, the bell-shaped profile occurred in case of laccase activity. Sv1 showed high enzyme activity at broad range of pH. The optimum activity for ABTS was found at pH 4.0 whereas the optimum activity for guiacol and L-dopa was found at pH 8.0 and 9.0, respectively. The bell-shaped activity profiles with phenolic substrates can be ascribed mainly to two antagonistic effects: (a) the redox potential of phenolic substrates decreases with increasing pH, which results in a larger redox potential difference of substrate and T1 copper and thus in higher activity; (b) hydroxide ions bind at the trinuclear cluster and inhibit the oxygen reduction which reduces activities at high pH [15,16]. Generally, fungal laccases are active under acidic conditions [4] and only few bacterial laccases show activity in alkaline milieu [17]. For certain industrial processes like addition of laccase to washing powder, decolourization of waste waters, or treatment of Kraft pulps, where alkaline reaction milieus prevail, alkaline activity would be preferable.

1.3.2.2. Effect of temperature

Sv1 is almost fully active in the temperature range of 50° C–90° C, with

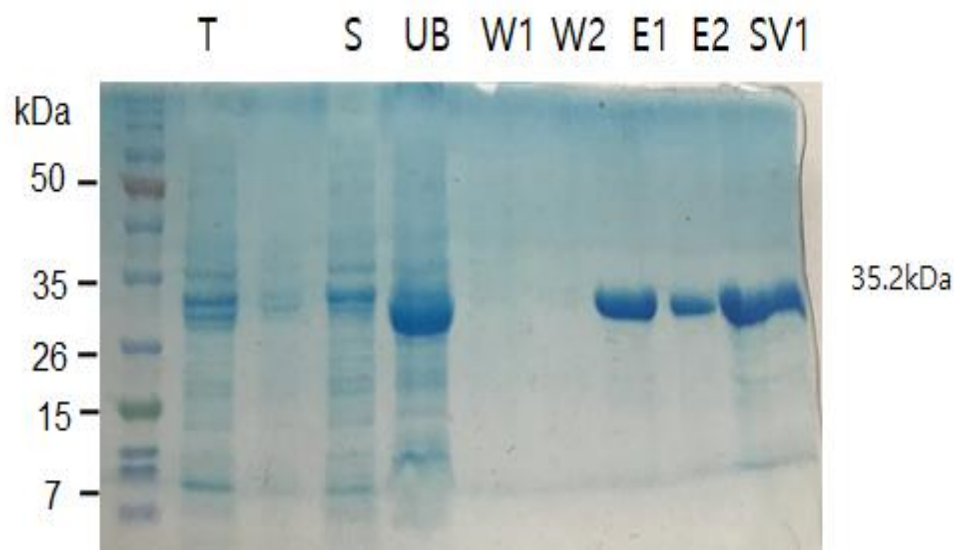

Figure 1.1 SDS page analysis of enzyme soluble expression and His-tag purification. Lanes; T, total expression; S soluble expression; UB, unbound fraction; W1/W2, wash-through fraction; E1/E2, Eluted fraction; Sv1, Concentrated enzyme solution

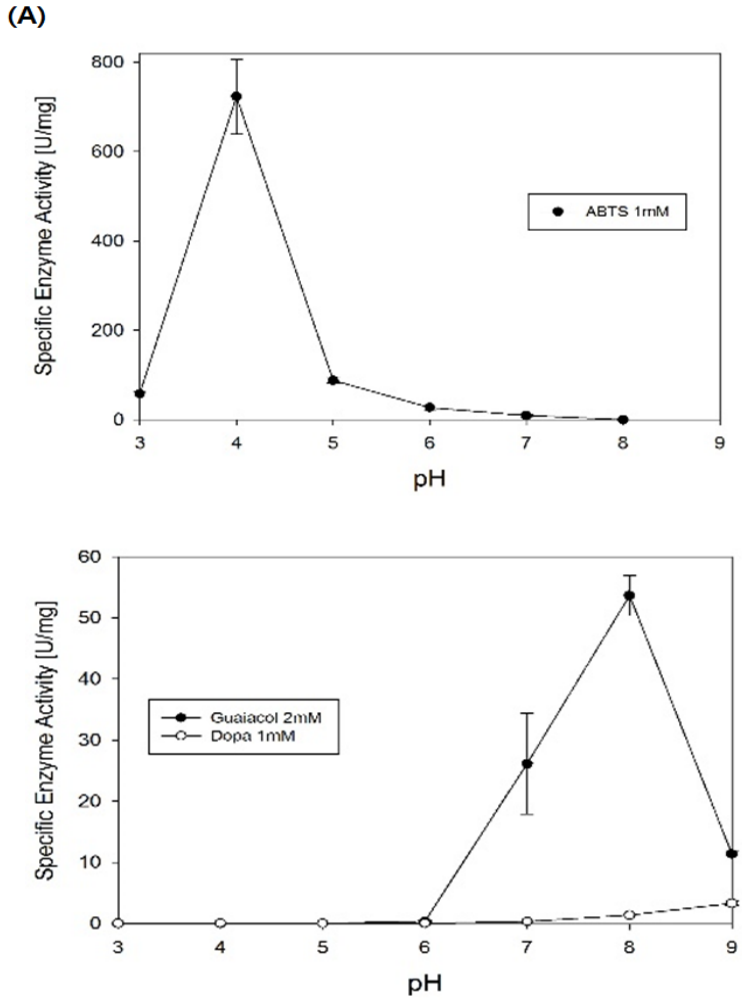

Figure 1.2 (a) Effect of pH on Sv1 activity. The specific enzyme activities were measured with three substrates (ABTS 1mM, guaiacol 2mM, L-dopa 1mM) around various pH conditions at room temperature without any addition of metal ions.

maximum activity at 70° C (Fig.1.2(b)). Pre-incubation of Sv1 at 60° C and 70° C greatly increased laccase activity. The activity remains unaltered after prolonged incubation at 40° C. Thermal stability is usually considered as beneficial for industrial processes since it is often connected to operational stability of the enzyme which allows higher reaction temperature, longer process duration, and in general a more flexible process management.

1.3.2.2. Effect of organic solvents

Relative activity of Sv1 in the presence of several organic solvents was examined. Presence of the water miscible organic solvents acetone, methanol (MeOH), ethanol (EtOH), and 1,4-dioxane did not alter activity of the enzyme (Fig.2(c)). With 50% MeOH, EtOH, and 1,4-dioxane in the reaction system, the activity dropped to 20 to 40%. However, the reactivity of Sv1 remained unchanged with up to 30 % of all the solvents. The maintained activity of Ssl1 with organic co-solvents allows use of the enzyme in a wide variety of reaction compositions. This is particularly useful since many described laccase substrates, like polyaromatic hydrocarbons or phenylpropanoids, are poorly soluble in water and use of an additional organic phase as substrate reservoir in the reaction could facilitate the conversion of higher amounts of substrate.

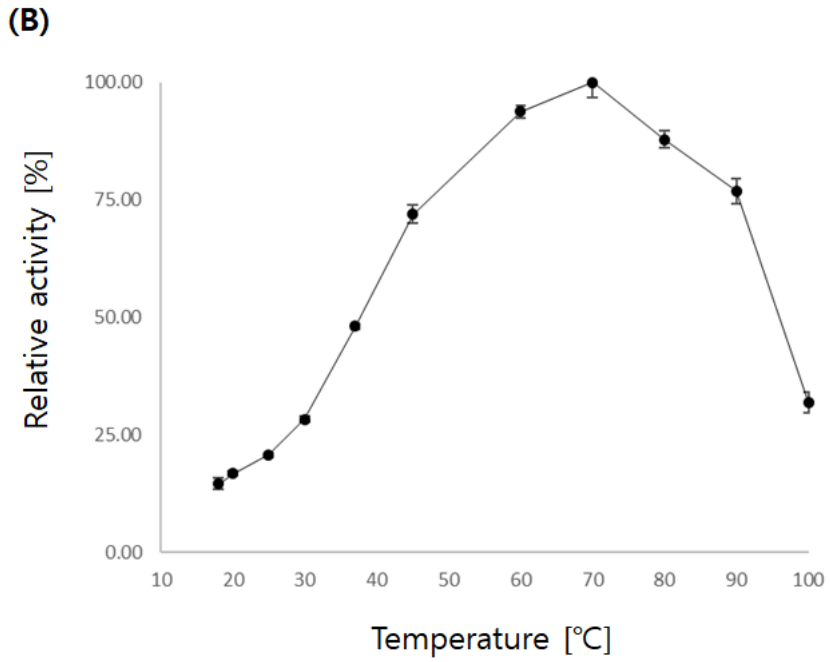

Figure 1.2 (b) Effect of temperature on Sv1 activity. The relative activities were measured with ABTS 1mM under various temperatures at pH 4 without any addition of metal ions.

(C)

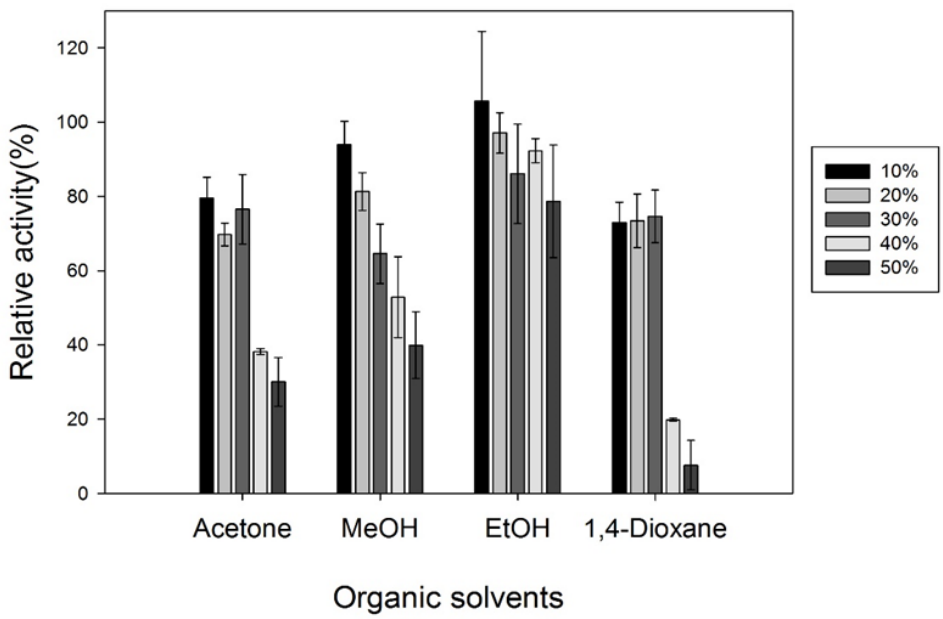

Figure 1.2 (c) Effect of organic solvents on Sv1 activity. The residual activity relative to that of control (without any organic solvent) were measured with ABTS 1mM at pH 4 and room temperature without any addition of metal ions.

1.4. Conclusion

Sv1 from *S. viridosporus* is a small two-domain laccase with unusual properties. It was able to be well expressed in *E. coli* and showed stability in a wide pH range, at elevated temperatures and in presence of organic solvents with a neutral activity profile. This makes Sv1 a suitable candidate for industrial biocatalysis, especially in processes that cannot be accessed by other laccases due to the requirement of high pH values or organic co-solvents.

Chapter II

Laccase catalyzed dimerization of eugenol oxide for potential polyol extender of robust, self-healable polyurethane elastomer

2.1. Introduction

Polyurethane (PU) is a very versatile polymer, which is used as rigid and flexible forms, coatings, films, and other products. [18] According to *market and market*, PU foam market size was estimated by nearly USD 56.8 billion in 2018. In general, polyurethane is synthesized with urethane bond between diisocyanate and polyol. [19] The polyols that play an important composition of PU, are conventionally obtained from petrochemical crude oils and coals. Petroleum based polyol causes serious environmental problem and depletion of natural resource. Another issue in PU synthesis is increasing biological contents regarding eco-friendly polymer production and environmental regulations such as REACH (registration, evaluation, authorization, and restriction of chemical). According to U.S Department of Agriculture and U.S Department of Energy, the goal of bio-based material is increase to 25 % in commodity chemicals and materials until 2030. [20] Recently sustainable and reusable polyurethane is getting attention and bio-based polyol is promising substitute of petrochemical polyol. [21] Natural oil polyols (NOPs) are being researched to produce environmentally friendly PUs because they are derived from vegetable oils such as crop asters with an aliphatic long chain structure. [22-24] Another approach demonstrated here is to use lignin derived phenolic compounds as a chain extender replacing widely used 1,4-butanediol. [17]

Lignin is the most abundant aromatic polymers composing lignocellulosic biomass. [25] Aromatic derivatives of lignin can be used as polyols or polyol chain extenders in PU synthesis. The aliphatic or phenolic hydroxyl group in lignin determines polyol reactivity with isocyanate and poor solubility, impurity, and polydispersity decrease the reactivity. Therefore, general strategies for incorporating lignin into PU are to increase the reactivity by converting it into aromatic monomers and increasing the hydroxyl content. [17] Lignin-derived vanillin [17], guaiacol [26], eugenol [27], creosol [28], and other phenolic derivatives have been successfully incorporated into PU production. Our groups demonstrated dimeric vanillin-based chain extender having structural rigidity to PU elastomer such as high transition temperature, high Young' s modulus, and high stiffness. [17] In this study, we expanded previous research into developing another lignin-monomer polyurethane elastomer with other specific properties. Eugenol has similar structure with vanillin but it has a distinct terminate alkene, which allows it to functionalize different from other lignin-based monomers. [29]

Eugenol (4-allyl-2-methoxyphenol) is obtained from lignin pyrolysis [30] and mainly from clove oils. [31] Under mild catalytic pyrolysis conditions, eugenols were produced about 10 wt % of from bio-crudes. [32] Eugenol is regarded as a prototypical lignin-derived compound for containing several key functional groups of lignin, which include methoxy, hydroxyl, and alkenyl on its aromatic body skeleton. [33] Interesting features of eugenol are a pleasant scent and excellent

antimicrobial activity, so that it may help avoid the odor problem and microorganism-induced damage in bio-based PUs. [34,35] Eugenol-based PU has enormous potential for applications in the biomedical approach such as eugenol-polypropylene with antibacterial effect. [36]

In addition, eugenol-based PUs newly stand a chance of being a promising engineering material with its self-healing effect. [37-40] Self-healing slight damages can meet requirements under special systems such as implanted medical devices, aerospace materials, and protective materials in dangerous places. [40] The self-healable properties will extend life span, improve reliability during applications, reduce wastes, and conform to requirements of sustainable development. [41] It is generally accepted that reversible bond between phenolic group in eugenol and isocyanate may dedicate to self-healing effect in polyurethane. [42] For example, Jing-yu Liang et al. designed a copolymer of eugenol terminated PU prepolymer and exhibited self-healing. [27] However, its functional phenol group has been found to be less reactive to be directly integrated into PUs. [42]

One way to facilitate the utilization of eugenol in PU synthesis is to attach terminal reactive groups to the phenolic group of eugenol, and there has been extensive research regarding the chemical modification of eugenol. [28,29,30] For example, eugenol was converted to mercapto-terminated oligomer [28], terminal diene derivative [29], copolymer with soybean oil [40], etc. to subsequently prepare polymers.

However, although eugenol-derived PUs have undergone extensive development, there are no available method to generate the eugenol-based PU containing free phenolic groups.

Herein, we present a novel eugenol-based polyol extender, dieugenol-hexaol conjugate (DE-hOH). DE-hOH is a symmetric hexaol compound that has two phenolic and four aliphatic alcohols so that it can impart structural rigidity and self-healing capacity to the final PU product (Fig. 3). This compound enables a rare example of eugenol derivative containing different reactive primary, secondary and phenolic hydroxyl groups (primary > secondary > phenolic). More reactive primary and secondary hydroxyl groups participate in urethane bond while leaving phenol group unreacted. To obtain this function, we first synthesized vanillyl diol and then dimerized it into symmetric configuration, which has a phenol and two alcohol groups on each end of the unit extender (Fig.2.1). Herein, eugenol-based polyol chain extender for PUs has been successfully synthesized with green enzymatic reaction and catalyst chemical reaction. This DE-hOH has been applied as hard segment of PU replacing the portion of 1,4-butane diol to enhance the characteristics of PU as presented in Fig.2.1 DE-hOH based PU was characterized by self-healing property.

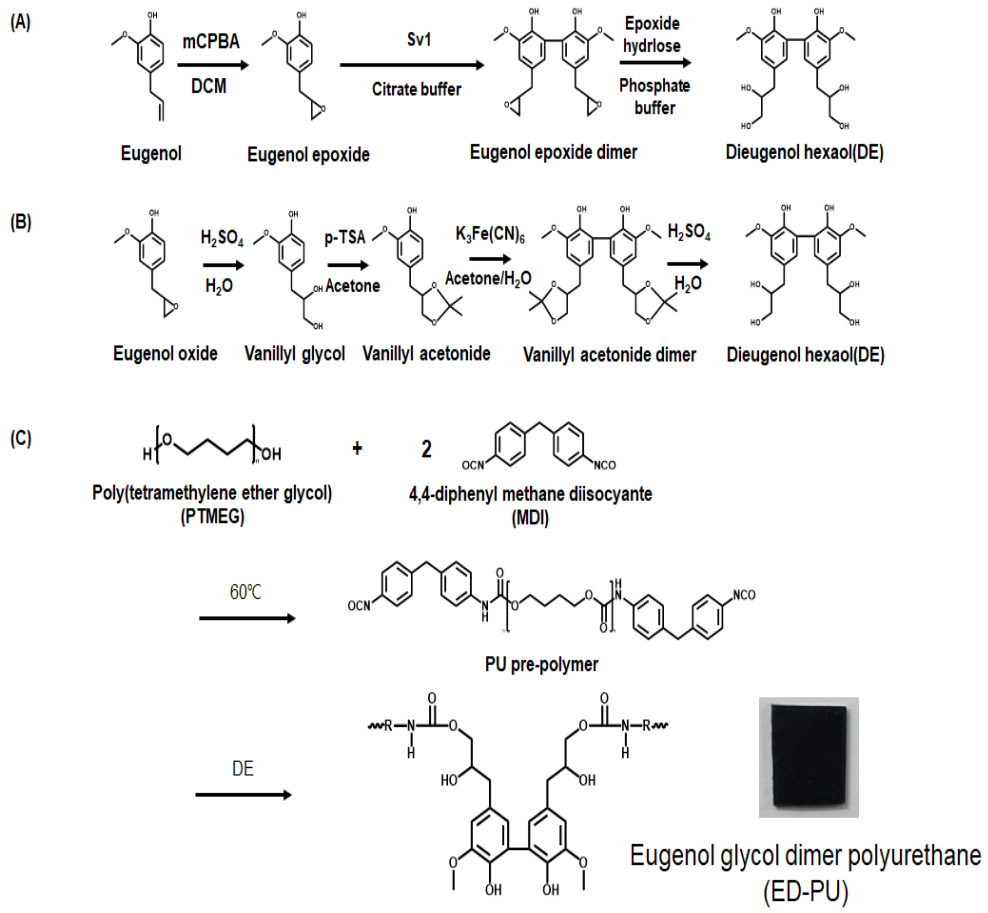

Figure 2.1. Overall scheme of synthesis steps for eugenol-based polyurethane elastomer. (A) Enzymatic synthesis, (B) Chemical synthesis of dieguenol-based hexaol(DE), (C) preparation of eugenol-based PU film.

2.2. Materials and methods

2.2.1. Chemicals and materials

All chemicals were of analytical grade and used as received; eugenol (Sigma, 99 %), m-chloroperbenzoic acid (Acros organics , 77 %), sodium sulfite (Junsei), sodium sulfate (Tedia) H_2SO_4 (Acros), sodium bicarbonate (Junsei), laccase from Trametes versicolor (Sigma, 0.92 U/mg^{-1}), 4,4′-methylene diphenyl diisocyanate (MDI), poly(tetramethylene ether glycol) (PTMEG) (Number average molecular weight (M_n) = 2,000 g/mol), and 1,6-hexanediol (HD) were purchased from Sigma Aldrich (Yong-in, Korea). MDI was used without any purification and PTMEG and HD was dried under vacuum at 70 ℃ for 24 h before use. N,N′-dimethylformamide (DMF) was used as a solvent in PU preparation.

All commercially available solvents (GR grade) or reagents were used without further purification unless otherwise noted. Reactions were monitored by thin layer chromatography (TLC) using pre-coated silica gel plates from Merck (TLC Silica gel 60 F254, 250 μm thickness). Flash column chromatography was performed over Silica gel 60 (particle size 0.04- 0.063 mm) from Merck from Sigma-Aldrich.

NMR spectra were recorded on Bruker Advance III 400 FT-NMR

spectrometer using residual solvent peaks as an internal standard (DMSO-d6 @ 2.50 ppm 1H NMR). The following abbreviations (or combinations thereof) were used to explain the multiplicities: s = singlet, d = doublet, t = triplet, q = quartet, m = multiplet, br = broad. All the intermediates and the product were derivatized with N,Obis(trimethylsilyl)trifluoroacetamide (BSTFA) at 50° C for 5 min and were analyzed with a gas chromatograph-mass spectrometer (GC-MS) equipped with an electron impact (EI) ionization source for identification according to a previously described method [25], with some modifications. The GC oven temperature started at 65° C, was held for 5 min, and then increased by 3° C/min to 250° C, with holding for 10 min. The ionizing electron energy was 70 eV, and the collected mass range was 150 to 1000 atomic mass units (amu).

2.2.2. Synthesis of dieugenol-based hexaol

2.2.2.1 Synthesis of Eugenol epoxide

Eugenol (5.3 g, 32 mmol) was dissolved in dichloromethane (100 mL), to which was then added dropwise a solution of *m*CPBA (11.15 g, 55 mmol) in dichloromethane (100 mL). The solution was poured into an excess of ice-water for 30 min and stirred at room temperature for 12 hours.

The reaction mixture was poured into an excess of ice-water, and then precipitated *m*CBA was filtered by vacuum filter with 0.45 μm membrane filter. The resulting mixture was worked up with aqueous 10 % sodium sulfite 200mL to neutralize the oxidizing agent. The organic phase was washed twice with aqueous sodium bicarbonate, once with brine, and dried on anhydrous sodium sulfate. After filtration, the filtrate was condensed to remove solvent, and the residue was further purified on a silica gel column (hexane/ethyl acetate = 20:1, v/v) to obtain the epoxide intermediate as a light yellow oil [3.2 g; 55 %].

2.2.2.2 Enzymatic synthesis of Dieugenol-based hexaol (2 steps)

Eugenol oxide (3.0 g, 17 mmol) was dissolved in 360 mL of citrate buffer and 40 mL of acetone. 40 U of Laccase from *Streptomyces viridosporus* T7A (*Sv*Lac) was preincubated at 30 ℃ for 10 min and mixed with the prepared eugenol oxide solution. After 24 hours of stirring at room temperature, the reaction mixture was filtered by vacuum filter with 0.45 μm membrane filter. The filtered cake (3.7 g, 7.4 mmol) was washed three times with distilled water.

The recombinant *E.coli* BL21(DE3) harboring the epoxide hydrolysis gene from *Mugil cephalus* and *Caulobacter crescentus* were

induced with IPTG 0.1 mM at OD_{600} reaching 0.6 and incubated at 18 ℃ for 24 hours. The cells were harvested and washed once with phosphate buffer. Then, the cells were preincubated in 333 mL of phosphate buffer and 37 mL of acetone at 30 ℃. The epoxide hydrolysis reaction was initiated by adding the filtrate into the pre-incubated cells and carried out at 30 ℃, 200 rpm for 24 hours. The aqueous solution was extracted three times with EA, twice with DE, dried on anhydrous sodium sulfate. After filtration, the filtrate was condensed to remove the solvent. The residue was further purified on silica gel column (dichloromethane/methanol = 20:1, v/v) to obtain the hexaol product as a brownish oil [3.4 g, 75 %].

2.2.2.3 Synthesis of Vanillyl glycol and its acetal protection

Eugenol oxide (40 g, 222 mmol) was dissolved in DCM (400 mL) and treated with 400 mL of water and 200 mL of 5 % H_2SO_4 solution. The solution was stirred at room temperature for 24 hours, and then dichloromethane was removed by evaporation. The aqueous solution was extracted three times with EA, twice with DE, dried on anhydrous sodium sulfate. After filtration, the filtrate was condensed to remove solvent, and the residue was further purified on silica gel column (dichloromethane/methanol = 20:1, v/v) to obtain the glycol intermediate

as a yellowish orange oil [31 g, 67 %].

Then, vanillyl glycol (30 g, 151 mmol) was dissolved in a mixture of acetone (600 mL, 542 mmol) and 5 mol % *p*TSA. Also, anhydrous $MgSO_4$ (50 mg) was added to remove any residual water. The mixture was stirred at room temperature until complete conversion was monitored by TLC. The resulting mixture passed through a silica gel for removal of the remaining *p*TSA and $MgSO_4$. After filtration, the filtrate was evaporated under reduced pressure, and the obtained product was the acetonide intermediate as a light yellowish brown oil [35 g, 98 %].

2.2.2.4 Chemical dimerization of Vanillyl acetonide and its acetonide deprotection reaction

Vanillyl acetonide (35 g, 147 mmol) was dissolved in acetone (450 mL) and water (225 mL), to which was added, to which was added 25 % NH_4OH (300 mL) and the mixture was stirred for 10 min. A saturated aqueous solution of $K_3Fe(CN)_6$ (47 g, 154 mmol, 1.05 eq.) was then added dropwise to this solution over 3 hours. More NH_4OH (300 mL) was then added to maintain the alkalinity in the reaction solution, and the mixture was stirred overnight at room temperature. After TLC indicated the complete consumption of the reactants, the volatile component was removed by evaporation. The aqueous solution was extracted three times

with EA, twice with DE, dried on anhydrous sodium sulfate. After filtration, the filtrate was condensed to remove the solvent. The residue was further purified on silica gel column (hexane/acetone = 3:2, v/v) to obtain the acetonide dimer as a brownish yellow oil [16 g, 47 %].

Vanillyl acetonide dimer (16 g, 34 mmol) was dissolved in ether·HCl (mL) and water (mL) and the mixture was stirred for 3 hours. After TLC indicated the complete consumption of the reactants, the reaction mixture was condensed to remove the solvent. Then, the residue was freeze-dried overnight to obtain the hexaol product as a brownish oil [12 g, 87 %].

2.2.3. Synthesis of polyurethane films

Two types of PU films with different chain extenders (HD and DU) were prepared by using prepolymer method. First, PTMEG (1 mol) and MDI (2 mol) was weighted into a four-neck round-bottom flask and the temperature was allowed to increase at 50 ℃ to obtain a homogeneous mixture. The reaction was carried out at 60 ℃ under nitrogen atmosphere until the NCO% was reached at the theoretical value. The NCO% was determined by back-titration method followed by ASTM D 1638-74. Then, the PU prepolymer was dissolved in DMF and the stoichiometric amount of chain extender (1 mol of HD or DU) was added to the PU prepolymer. In this work, DU was regarded as a diol although it has the six hydroxyl

groups in its molecules to remain the free hydroxyl groups. After 3 h, the solution was poured into a Teflon mold and placed in a convection oven set at 110 ℃ for 1 day to remove the solvent. The PU films prepared by using HD and DU as a chain extender were named as CPU and DPU, respectively. The flow chart for the preparation of PU films were presented in Table 1.

2.2.4. Characterization of polyurethane films

Fourier transform infrared (FTIR) was used to confirm the chemical structure of CPU and DPU by employing FTIR spectroscopy (FTIR 4600, JASCO). The FTIR spectra of PU films were obtained using attenuated total reflectance (ATR) accessory at a resolution of 4 cm^{-1} at room temperature. The thermal properties of both PUs were carried out using differential scanning calorimetry (DSC) (Q20, TA instrument). About 5 mg of sample was sealed in a platinum pan and measured at a heating rate of 10 ℃/min with nitrogen atmosphere. The dynamic mechanical properties of CPU and DPU were investigated by employing dynamic mechanical analyzer (DMA) (Q800, TA instrument). The sample with the dimension of 15 mm × 5.3 mm × 0.7 mm (length × width × thickness) was measured ranging from −100 ~ 200 ℃ at a heating rate of 5 ℃ /min. The tensile properties and self-healing efficiency of PU films were investigated employing a universal testing machine (UTM) (LR5K Plus,

LLOYD). The crosshead speed was controlled at 500 mm/min. The four specimens with dog-bone-shape per samples were measured and averaged to obtain the representative data.

2.3. Results

2.3.1. Preparation of dieugenol-based hexaol

To provide primary, secondary, and aromatic hydroxyl group in polyol, we focused on dieugenol-based hexaol. Dieugneol-based hexaol has never been reported in academia. To synthesis dieugenol-based hexaol from eugenol, we have established 3-step routes *i.e* eugenol epoxide, its dimerization, and ring opening (Fig.2.1). First, epoxidation of eugenol was progressed by 3-chloro-benzoic acid (mCPBA) reagent with eugenol, thereby resulting in epoxide group at the alkene of eugenol. Secondary, 0.1 U/mL of laccase directly formed C-C bond at C5 and C5' position of the eugenol oxide (41.6 mM) in high yield (87 %) under pH 5 buffer solution. Finally, eugenol epoxide dimer undergoes hydrolysis of epoxide to diols by sulfuric acid. The products of each step were characterized by ^{1}H-NMR and GC MS.

Table 2.1. Composition of PU films

Sample code	Compositions (by mole ratio)			
	PTMEG 2000	MDI	HD	DE
Control-PU	1	2	1	-
EDH-PU	1	2	-	1

However, enzymatic reaction has some limitations such as solubility of eugenol epoxide in buffer and unstable epoxide ring structure in aqueous condition. We have detoured the routes to produce eugenol-based hexaol to make large scale reaction. First reaction is the same as previously described and then hydrolysis of epoxide reaction is followed to prevent generating byproducts from reactive epoxide and keeping compound longer. Vanillyl glycol was not feasible to dimerize directly by radical reaction because of interference between diol. Reactive diol was protected with acetal group through p-Toluene sulfonic acid (p-TSA). The protecting acetal groups were removed after dimerization with treatment of an aqueous acid catalyst. The overall yield of dimerization throughout the whole processes was ca. 40 %. In summary, epoxide product is rapidly transformed into glycol formation to prevent side reaction and dimerization step altered with iron catalyst ($K_3Fe(CN)_6$) to overcome drawbacks in solubility of eugenol epoxide.

First, two alcohol functional groups at C1 position of each propenyl group were introduced using hydroxylating agents, thereby resulting in three alcohol moieties in eugenol backbone. 3-chloro-benzoic acid regioselectively oxidized the alkene group of eugenol, and then aqueous acid was added to open the epoxide ring. By modifying the processes referred to as, overall yield of 160 mM of eugenol reacted improved up to 34 % (Fig.2.2). The intermediate eugenol oxide

and vanillyl alcohol were characterized ^{1}H-NMR spectrum and GC-MS in figure 2.2.

Secondly, 0.1 U/mL of laccase directly formed C-C bond at C5 and C5' position of the eugenol oxide (41.6 mM) in high yield (87 %) under pH 5 buffer solution. However, the enzymatic reaction has some disadvantages over chemical methods in large-scale, *i.e.* poor solubility of eugenol oxide in buffer and high cost of enzyme. To overcome these drawbacks, we additionally used $K_3Fe(CN)_6$ as a catalyst of the radical dimerization because it provided low price and mild reaction condition even in large-scale. $K_3Fe(CN)_6$ catalyst can't directly dimerize the eugenol oxide and vanillyl alcohol at all, so we had to block the primary and secondary alcohol groups in the vanillyl alcohol so as to circumvent the problem of their interfering $K_3Fe(CN)_6$ catalyst. The protecting acetal groups were removed after dimerization with treatment of an aqueous acid catalyst. The overall yield of dimerization throughout the whole processes was ca. 40 %. The final product DE-tOH was characterized by ^{1}H-NMR and GC-MS analysis as shown in Figure 2.2.

2.3.2. Chemical identification of polyurethane films

The following results were conducted by Shin sera, Conbuk national university. The Chemical structure of PU films was confirmed by employing FTIR spectroscopy, and the FTIR spectra are present in Figure 5. The peak appearing at 2270 cm^{-1} in FTIR spectrum of prepolymer corresponds to the isocyanate (NCO) functional group. NCO functional groups were not detected in FTIR spectra of EDH-PU and CON-PU, implying that the chain extension using DE and HD was successfully performed. In FTIR spectra of EDH-PU and CON-PU, the characteristic peaks of urethane unit were commonly observed at 3297 cm^{-1} (N–H stretching), 1733 cm^{-1} (urethane C=O), 1538 cm^{-1} (N–H bending), and 1602 cm^{-1} (aromatic ring). As a result, it was confirmed that EDH-PU has pendant hydroxyl groups in its molecular structure. This pendant hydroxyl groups are designed to participate in the exchange reaction with carbamate groups for self-healing of PUs.

2.3.3. Properties of eugenol-based polyurethane elastomer

2.3.3.1. Self-healing property of the polyurethane elastomer

In this study, the exchange reaction of pendant hydroxyl groups (secondary and phenolic hydroxyl groups in EDH with carbamate groups can impart self-healing properties of PUs. Self-healing properties were

(A)

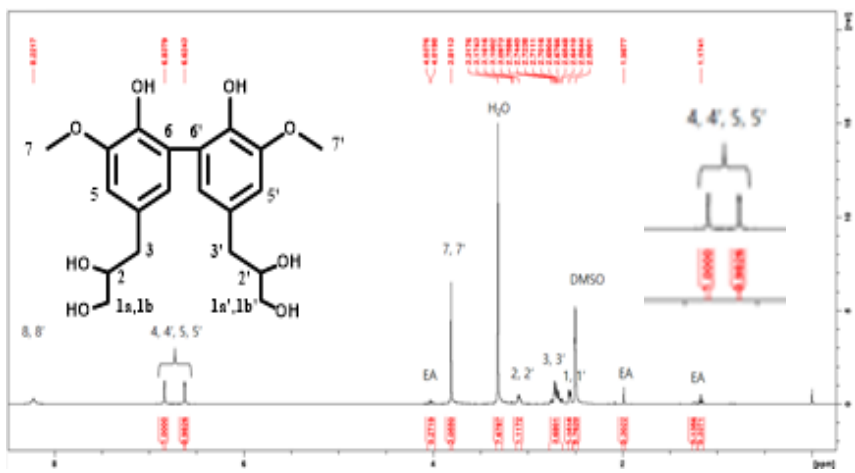

Figure 2.2. (a) ^{1}H NMR result of dieugenol-based hexaol product.

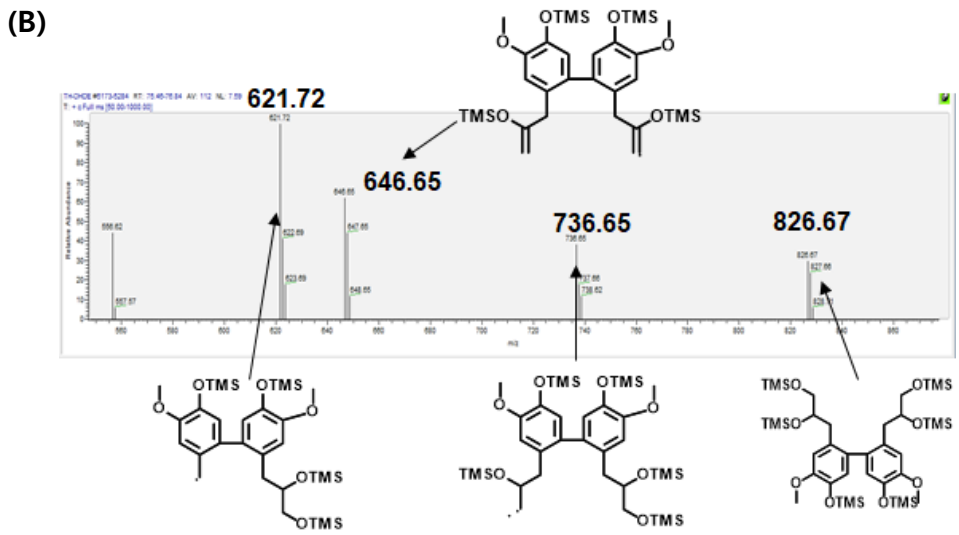

Figure 2.2. (b) GC-MS/MS fragmentation pattern of dieugenol-based hexaol product.

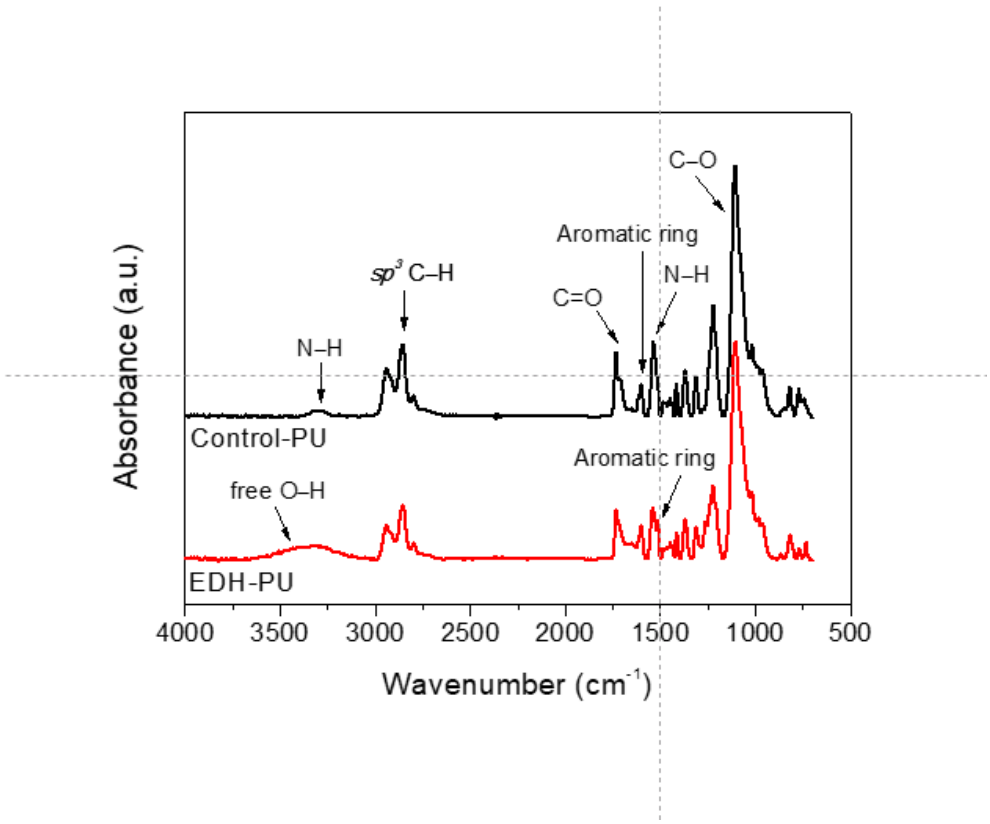

Figure 2.3. FT-IR result of polyurethane films. PU-HD was constructed as control film.

investigated by using tensile test. Self-healing efficiency was calculated according to the following equation.

$$\text{Self-healing efficiency (\%)} = \sigma_{\text{healed}} / \sigma_{\text{original}} \times 100\%$$

$$\text{Self-healing efficiency (\%)} = \frac{\sigma_{\text{healed}}}{\sigma_{\text{original}}} \times 100\%$$

where σ_{original} corresponds to the tensile strength of sample before self-healing and σ_{healed} indicates the tensile strength of sample after self-healing at 150 ℃. It was found that EDH-PU with pendant hydroxyl groups capable of exchange reaction exhibited excellent self-healing performance. It can be inferred that this is mainly due to the configuration change by the exchange reaction between the free hydroxyl groups and urethane group.

2.3.3.2. Other physical properties of the polyurethane elastomer

The thermal properties of EDH-PU and CON-PU were investigated by employing DSC (Fig. 2.4). The endothermic peak around −75 ℃ corresponds to the glass transition temperature (T_g) of soft segment of PUs, and EDH-PU and CON-PU showed the similar T_g. In addition, the melting temperature of the PTMEG was observed at 10.8 ℃ for EDH-PU and 14.7 ℃ for CON-PU. It means that the glass transition of the

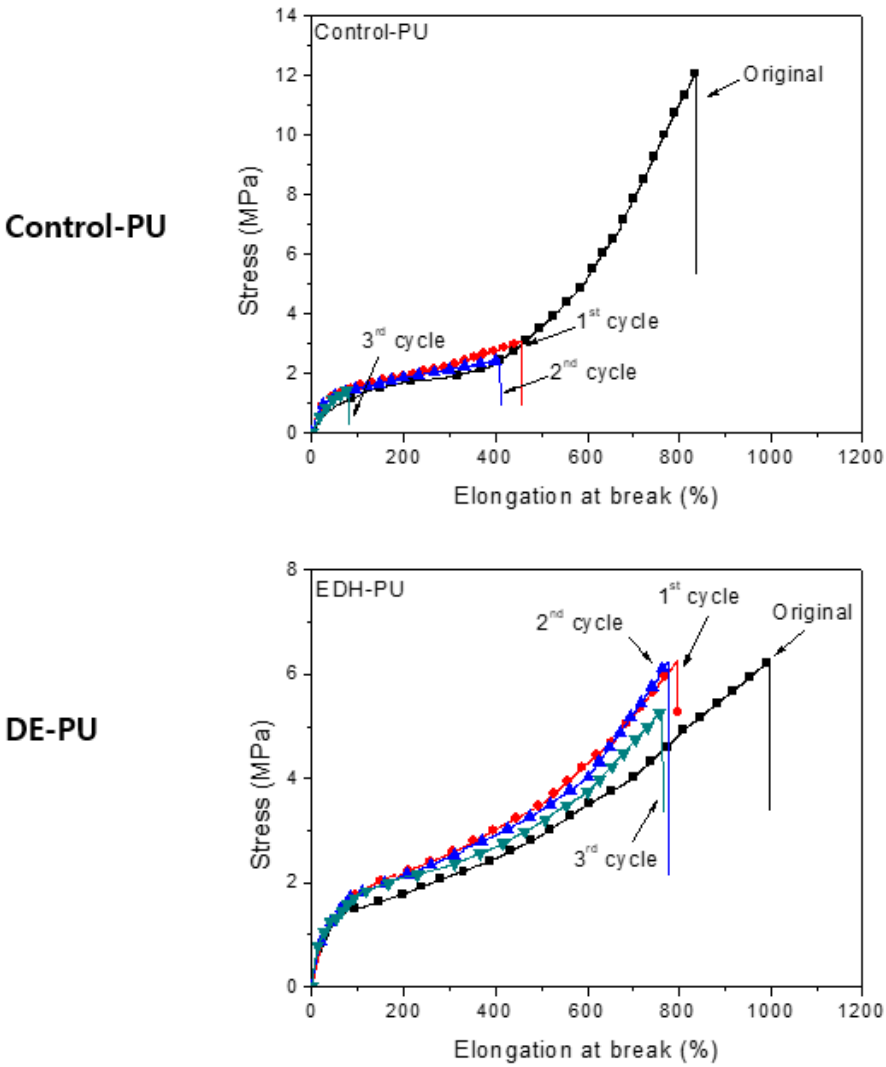

Figure 2.4. Self-healability test of eugenol-based polyurethane. Serial tensile tests after self-healing were carried out to measure self-healing efficiency. PU-HD was constructed as control-PU.

amorphous phase was not clearly observed as the crystallization of the soft segment of EDH-PU increased. Figure 2.5 shows stress-strain curves of EDH-PU and CON-PU. EDH-PU exhibited a slightly higher Young's modulus compared with CON-PU due to the introduction of more aromatic ring in the hard segment of PU. However, the tensile strength of EDH-PU was almost half that of CON-PU. The bulky DE can weaken the micro-phase separation by interfering with the packing of hard segments, and the pendant hydroxyl groups can also inhibit the micro-phase separation by the formation of hydrogen bonds.

2.4. Conclusion

In this study, bio-based eugenol derivatives were successfully synthesized and introduced to PU production as a chain extender. Of the six hydroxyl groups, only two primary hydroxyl groups were designed to participate in the chain extension and the remaining hydroxyl groups (secondary and phenolic hydroxyl groups) were used to provide self-healing and antioxidant properties. Free hydroxyl groups in EDH-PU were confirmed in FTIR spectroscopy, EDH-PU exhibited the comparable thermal properties including glass transition temperature compared with CON-PU. EDH-PU chain-extended with bulky aromatic rings showed higher Young's modulus and lower tensile strength compared with CON-PU, which was

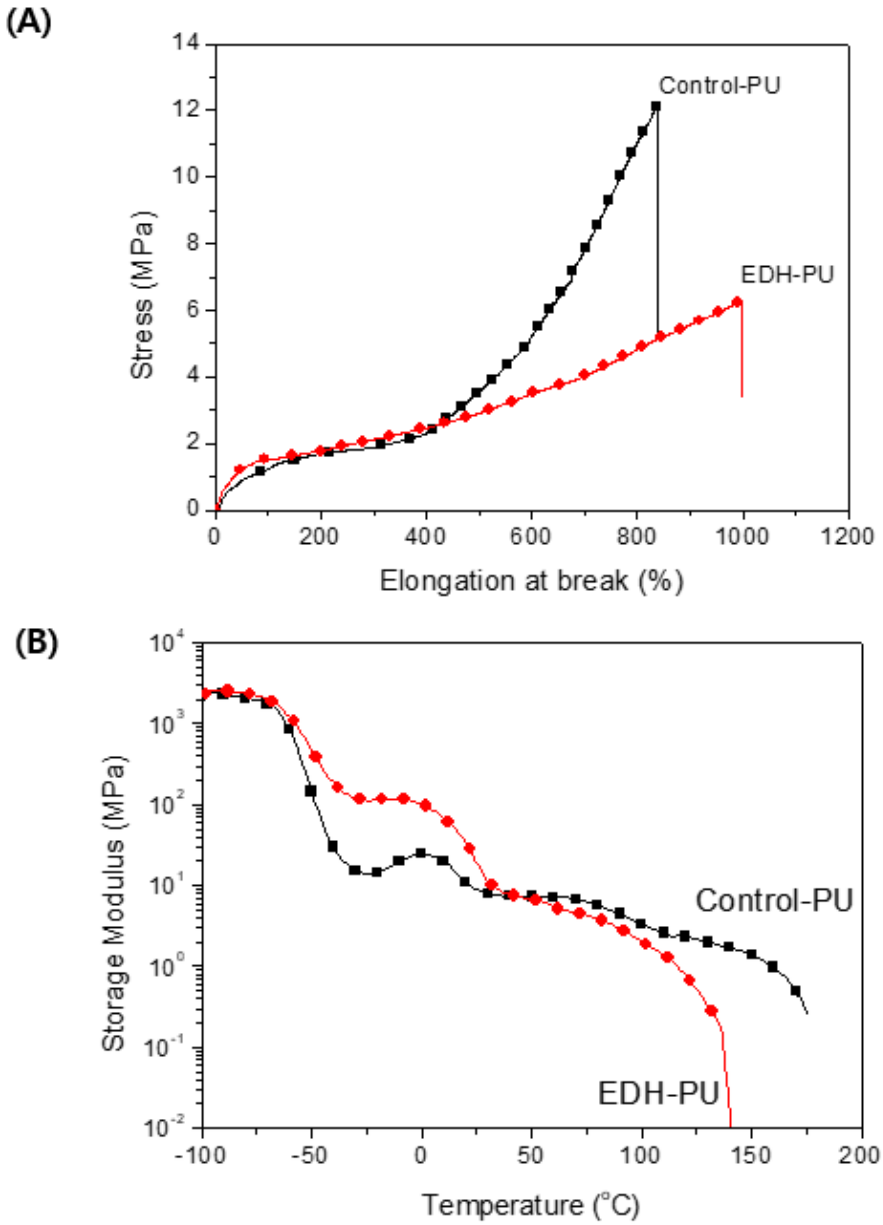

Figure 2.5. Other physical properties of eugenol-based polyurethane elastomer. (a) Tensile test and (b) DSC analysis of polyurethane films

attributed to the result of lower micro-phase separation between the soft segment and hard segment in PU. It was found that EDH-PU also has excellent self-healing properties induced by the exchange reaction of free hydroxyl groups with carbamate groups. It was postulated that EDH synthesized in this study can be a potential bio-based raw material capable of self-healing and antioxidant activity to prolong the life of the polymers.

Chapter Ⅲ

Laccase mediated one-pot dyeing of wool fabrics using recombinant *Streptomyces glaucescens*

3.1. Introduction

The conventional dyeing method usually involves the use of chemical auxiliaries and operates at the elevated temperature to assist the dye diffusion and fixation. For example, the coloration of wool fabrics should be co-treated with metal auxiliaries (Al, Cr, Fe, As) under acidic conditions. [41] However, the dyeing industry daily lets out 1-3 kilotonnes of water effluents rich in dyes and metal agents, accounting for 17-20 % of total water contamination. The long-term or accidental exposure to it can cause health problems from skin irritation to adverse health effects such as neurotoxicity and cancer. [42] Therefore, we need to develop a non-toxic and sustainable dyeing method. There have already investigated ultrasonic dyeing method and supercritical CO_2 dyeing method, yet they encountered several limitations in industrial scale operations, such as high construction cost and poor reproducibility. [43,44] To overcome these issues, several methods of biological dyeing, which use natural dyes without the use of chemical opponents have been developed. [45] The sources of natural dyes and their productions are biodegradable and renewable. Moreover, the enzymatic processes for dyeing can be working under normal conditions of temperature, pH, and pressure. Indeed, biological dyeing systems are safe, and they need less water for washing than chemical dyeing systems, resulting water conservation.

Laccase, a type of phenol oxidase, can oxidize a variety of phenolic compounds including flavonoid and catechol to form oligomeric chromophores. [46] The laccase reaction involves one electron, radical oxidation of substrates, concurrently with reduction of oxygen into water molecule. These free radicals may further react with not only substrate itself but also reactive groups in textile, so that the oligomeric products can be absorbed or fixed upon the textile. [47,48]

Mussel-inspired coating materials have received great attention because such dopamine derivatives are easy to obtain highly adhesive properties to various materials. Among them, oxidation of dopa, resulting in melanin, can be used as an economical source of dye due to its easy obtainability and low price. [49] W.Jia et al. showed that laccase from Trametes versicolor was able to be used for polymerizing dopa to strongly colored solution, resulting a dyed-silk fabric [50]. However, the dyed fabric showed low drop-off value on the color fastness test, indicating insufficient covalent bonding between melanin and silk. [50] Indeed, conventional studies used commercial laccases, causing a limitation on further large-scale dyeing process. [46,47,48,50] Majid Montazer et al. (2009) found that the application of purified laccase (Denilite II S) enhanced the color depth of wool fabrics in that laccase modified physical properties of wool fabrics before dyeing fabrics with madder. [51] Also, Jeon et al. (2010) studied that *T. versicolor* laccase catalyzed polymerization of natural phenols derived from edible plant fibers for polymeric dye in further hair dyeing. [52]

Here, we developed a novel one-pot method for simple and convenient coloration of wool fabric. We obtained both laccase and melanin from cultivated cells, and directly used the cell-culture media for dyeing. We transformed melanin-secreting *Streptomyces glaucescnes* (*S.glaucescens*) with a vector that codes for a heterogeneous laccase from *Streptomyces viridospours* (*S.viridospours*) (scheme 1a). We optimized an inducer concentration as well as an induction stage on laccase expression and confirmed the yield and activity of laccase by performing SDS-PAGE analysis and ABTS activity assay, respectively. The melanin secretion was confirmed by matrix assisted laser desorption/ionization (MALDI-TOF MS) and nuclear magnetic resonance (NMR) spectroscopy. Finally, laccase in the cell supernatant was used for catalyzing the coloration of melanin on wool fabrics. The K/S values of dyed wool fabrics were calculated, and their surface characterization was performed by fourier-transform infrared spectroscopy (FT-IR) and scanning electron microscopy (SEM).

3.2. Materials and methods

3.2.1. Cell culture conditions

Escherichia coli (E.coli) DH5α and JM110 for DNA cloning were grown in Luria-Bertani (LB) liquid broth or LB agar. Streptomyces viridosporus (S.viridosporus) T7A and Streptomyces glaucescens (S.glaucescens) NRRL

B_2706 (Korean Collection for Type Cultures) were grown on R2YENG agar plates for transformation then the proteins were expressed at 30 ° C for X h with 200 rpm shaking in R2YENG liquid media supplemented with 5 % (w/v) of fructose. Thiostrepton 2.5 μg/mL was added to the culture media depending of the plasmid used. DNA manipulations in Streptomyces were performed as described by Kieser et al.

3.2.2. Plasmid and strains construction

To construct the plasmid, PstS promoter from Streptomyces lividans (S. lividans) was amplified with the primers, 5'-ATATGAGCTCAGCCCCGGGACCG-3' and 5'-GGTGCGGCGTTCCATGCGCTGAAGCTTCACTTG-3', as well as a putative signal sequence of α-amylase gene (NZ_CP009438.1) from S.glaucescens NRRL B-2706 was amplified with the primers, 5'-GAAGCTTCAGCGCATGGAACGCCGCACCG-3' and 5'-ATATGGATCCTTCCGGCACGGCGTGCAG-3'. The probability of signal peptide sequence and its cleavage site were predicted using a neural network method-based SignalP server (version 4.1) (Petersen et al.2011). The amplified fragments were annealed to a single fragment by using overlap extension PCR. The PCR product was digested with restriction enzymes, SacI and BamHI, and then cloned into SacI- and BamHI -digested Streptomyces-E.coli shuttle vector pIBR25, resulting a plasmid that has a PstS promoter in-frame with α-amylase signal peptide.

The laccase ORF (GI 2518361192) was amplified from S.viridosporus T7A with primers, 5'-ATATGGATCCACCGGACCGGCGAAGAC-3' and 5'-AATATCTAGATCAGTGCGCGTGCTCCTCC-3'. PCR products were digested with SacI and BamHI, and cloned into SacI- and BamHI- digested plasmid X.

3.2.3. Protein expression

The activity of secreted Sv1 in the supernatant of liquid cultures of the wild type Streptomyces glaucescens NRRL B-2706 harboring the plasmid was determined as follows: Cells were grown for 200 rpm, 120 days at 30℃ in R2YENG medium supplemented with 0.5 % fructose and 2.5 μg/mL thiostrepton. Cell medium was spinned down (2,090 x g, 30 min), and the obtained cell supernatant was concentrated to ten-fold. The oxidase activity of the cell supernatant (Sv1) was measured using 1 mM ABTS substrate. The reactions of 200 μL reactant including 40 μL supernatant with 50 mM sodium acetate buffer (pH 4.0 were performed for 30 min at room temperature.

Reactants were placed into a polystyrene 96-well plate (Falcon 3690) and their absorbance intensities were measured by using UV spectrometer. Wavelengths and molar absorption coefficients used to measure oxidative activity as ABTS and ε420 = 36 mM-1 cm-1, respectively (Johannes and Majcherczyk, 2000). Reactions were performed in triplicate and were

initiated by adding 180 μL enzyme solution to 20 μL substrate. Controls without enzyme were also included.

3.2.4. Coloration of wool fabrics and color measurement

The wool fabrics were pretreated with distilled water for 10 min for improving its wettability. Then, the biological coloration of the wool fabrics was carried out in the following steps. (A) First, 2 mL of the cell medium was put in the buffer solution (50 mM pH 5 sodium acetate/ pH 8 sodium phosphate) 8 mL. Second, 0.25 g of the wool fabric was immersed in the reaction solution 10 mL. The reaction media was shaken for 200 rpm, 4 hours at 50 ℃. (B) First, 2 mL of the cell medium was put in the buffer solution 8 mL. Second, 0.25 g of the wool fabric was immersed in the reaction solution 10 mL. The reaction media was shaken for 200 rpm, 2 hours at 50 ℃. Then, 0.1 mL of 200 mM $FeSO_4$ solution was added into the reaction mixture, and the reaction resumed for another 2 hours at the same condition. The fabrics were washed twice with buffer and then with distilled water for 20 min.

The wool fabric samples were fold three times and measured using (Korea) at five different points. The range of wavelength was 360-740 nm. The levelness of coloration was determined by the average K/S value and relative standard value Sr(λ). Durability of pigment onto wool fabric was tested by the following procedures KS K ISO 105-C01: color fastness to domestic and commercial washing (scale 1-5).

3.2.5. Dye pigment and colored wool fabric analysis

Melanin was purified by centrifuging the fermentation broth at 5,000 x g for 30 min to remove both cells and debris. To precipitate the melanin, the pH of the supernatant was adjusted to 2.0 using 6 M HCl and then allowed to stand for 4 h. The precipitate was collected by centrifugation at 9,000 g for 15 min. Melanin pellets were washed with distilled water four times and centrifuged at 9,000 g for 15 min to obtain the purified pigment. Purified pigment was lyophilized and stored at -20 ° C until further use.

3.2.5.1 UV-visible spectrophotometric analysis

The purified melanin powder was dissolved in 50 mM NaOH solution and scanned in a UV–visible spectrophotometer (BMG Labtech, Germany) at UV, visible and near-infrared wavelengths (200–700 nm). The blank control was 50 mM NaOH solution without melanin powder.

3.2.5.2 MALDI-TOF MS

Mass spectrometry analysis was performed using Microflex MALDI-TOF MS (Bruker, Bremen, Germany). Ions formed by a pulsed UV laser beam (nitrogen laser, L = 337 nm) were accelerated to 15 keV. The analysis parameters were as follows: positive ion and reflectron mode, detector

gain = 3.9, and laser power = 40%. A total of 1200 shots from 6 different spots were scanned to obtain a mass spectrum. Lyophilized samples were analyzed under MALDI conditions. Samples were dissolved in 3 mg/mL of 50 mM sodium hydroxide solution. 0.5 μL of solution was mixed with 0.5 μL of DHB [2,5-dihydroxybenzoic acid] matrix solution (5 mg/mL in 30 % water/ 70 % acetonitrile [v/v]). 1 μL of the mixture was deposited on a stainless steel sample holder and allowed to dry before being placed in the mass spectrometer. Three independent MALDI-MS measurements were made for each sample, to evaluate reproducibility.

3.2.5.3 FT-IR spectroscopy

The FT-IR spectroscopic analysis was conducted on a FT-IR spectrometer JENSOR27(Bruker, Germany). The spectra were recorded in the range of 4000–500 cm^{-1} at a resolution of 4 cm^{-1} and 16 scans per sample.

3.2.5.4 SEM analysis

The wool fabric samples were scanned using a Scanning electron microscope JSM-7800F Prime (JEOL Ltd, Japan) that operated at 5.0 kV and had a magnification of 1.0 k to 10.0 k.

3.3. Results

3.3.1. Overexpression and secretion of laccase using a heterologous system in *Streptomyces glaucescens*

We constructed a pIBR25-based expression vector that codes an *e.coli* pUC origin, a replication region for *Streptomyces* from pIJ101, and a signal peptide sequence of amylase followed by a laccase-producing sequence. We used a partial sequence of heterogeneous laccase from *S.viridospours* due to its high thermal stability and wide range of pH dependency [53]. Sevillano et al., showed that a utilization of PstS promoter (PstSp), which drives transcription of the high-affinity phosphate-binding protein, enhances the secretion of heterogeneous enzyme in Streptomyces system [54]. Moreover, although a native signal peptide has used as a generic signal sequence for transporting non-native enzymes on the basis of an efficacious signal peptide-cleavage by its inherent signal peptidase [55], a native signal protein sequence in *S.glaucescens* has not been developed so far to facilitate the secretion of any heterologous protein. According to the data from signalP, it was expected that a signal peptide-cleavage site located at the N-termini of native α-amylase can be used for the expression of heterologous proteins. Indeed, it has been known that an intact signal peptide is essential for maturation and secretion of any heterologous protein [15]. To this end, we inserted a PstSp gene from *S.lividans* to the signal peptide, which is composed by 28 amino acids and subsequent three residues of mature α-amylase from *S.glaucescens* to obtain a high level of laccase expression.

We transformed melanin-secreting *S.glaucescens* with a laccase expression vector, and expressed laccase by adjusting the induction conditions. We cultured the cells in R2YENG medium for 5 days at 30C, and induced the expression of laccase with or without 5% fructose during one or two day(s). After collecting the cell supernatant, we confirmed the secretion level of laccase by performing an SDS-PAGE analysis (Fig. 8(a)). As a result, we successfully obtained a soluble laccase both for 1 day and for 2 days induction. It was confirmed that the addition of fructose was necessary to increase the yield of laccase expression, corresponding to a previous study showing that PstSp from S. lividans (AJ698727) was expressed in cultures containing glucose or fructose [16].

Next, we calculated the activity of extracellular secreted laccase via ABTS assay. The volumetric activities of extracellular laccase at the different induction conditions were calculated. Laccase expression vector-inserted cells, which were induced with fructose for 1 day and 2 days showed 1.12 U/L and 1.01 U/L of activity, respectively, while the activity of the cells without laccase expression vector and without fructose was 0.096 mU/L and 0.15 mU/L (Fig.3.1(b)). These results indicate that fructose has an efficiency, and the strong PstSp as well as the designed signal sequence promoted the secretion of activate laccase.

Interestingly, the melanin producing yield of transformed cell with laccase expression vector was 63.66%, which was lower than the control group; cells without laccase expression vector (100%) (Fig.3.1(b)). In order to examine whether the melanin was degraded by laccase, we mixed

melanin with purified laccase, and measured the absorbance using UV-vis spectrometer. As a result, laccase showed no influence on the melanin figment, suggesting that the melanin production was independent with laccase activity, and was improved with increased induction time.

Next, we varied the detailed induction conditions including the amount of inducer and induction stage to optimize the amount of laccase mordant and melanin dye. First, fructose concentration in the range of 0% to 5 % was tested and the results showed that the more concentration of fructose results the higher laccase activity (Fig.3.2(a)). After that, we confirmed the correlation between cell growth with 5% fructose and the melanin formation in five days. As a result, the cell culture showed a growth curve at the lag phase (day 0), the exponential phase (day 1), the transitional phase (day 2), and the stationary phase (day 3 and 4), which revealed that the strain was induced at the stage of day 1 (Fig.3.2(b)).

Interestingly, there was a correlation between the concentration of inducer and the amount of laccase secretion (R^2=0.9787) (Fig.3.2(a)).

Namely, a little laccase was secreted without fructose, which was partially due to the possibility that the remaining sucrose in the medium was degraded into the fructose. Besides, the increased inducer concentration was contributed to the decrease of melanin production as previously mentioned above. The strain produced 5.27 g/L of melanin figment, the amount of melanin produced by strain decreased into 61.39 % without induction, and 37.34 % with 5% inducer.

To confirm whether the induction stage affects the melanin production, we supplied fructose inducer in various growth phases. The cell density was highly correlated to the activity of extracellular laccase and to the production yield of extracellular melanin (Fig.3.2(c)). The induction at the exponential phase reached the optimum. Compared to the exponential phase, laccase was secreted at 22.87 %, 89.81 %, 60.25 %, 33.19 % of that when the cell was induced at the lag phase (day 0), the transitional phase (day 2), the stationary phase (day 3, 4) respectively. Except for the induction at day 0 and day 1, all groups generated more than 80 % of melanin production of cell with 5 % in the exponential phase. Especially, the group induced in the transitional phase produced the highest amount of the melanin (103.16 %) among four groups.

Taken together, the optimal induction condition was inducing the designed cell with 5 % fructose when the OD600 was between 2.5 and 3.0. This is mainly because the cell produced the highest amount of melanin when its laccase expression was induced. Time course of laccase secretion and extracellular melanin production by S. glaucescens (secretor tramsformant) gave clues to the optimal time point across the entire incubation, when the cell yielded 1.01 U/L of the extracellular laccase and 7.8 g/L of the extracellular melanin (Fig.3.2(c)).

3.3.2. Enhanced colorization of wool fabrics by the transformant

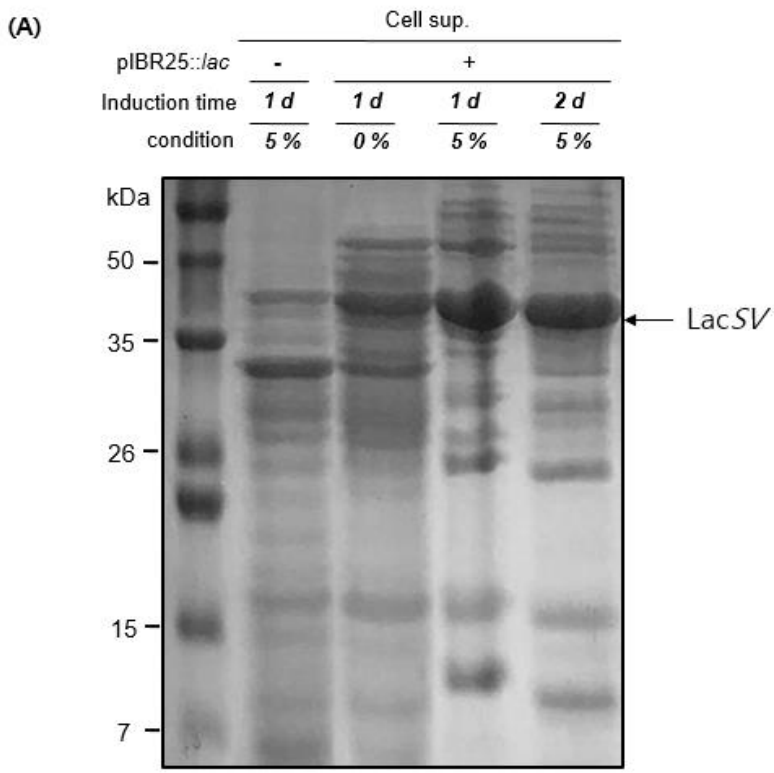

Figure 3.1. (a) A SDS-PAGE gel prepared from supernatants of S.glaucescens transformed. Each Sample was taken after 5 days of culture in R2YENG supplemented with 5 % fructose. 5 μL of supernatants were loaded in each lane.

(B)

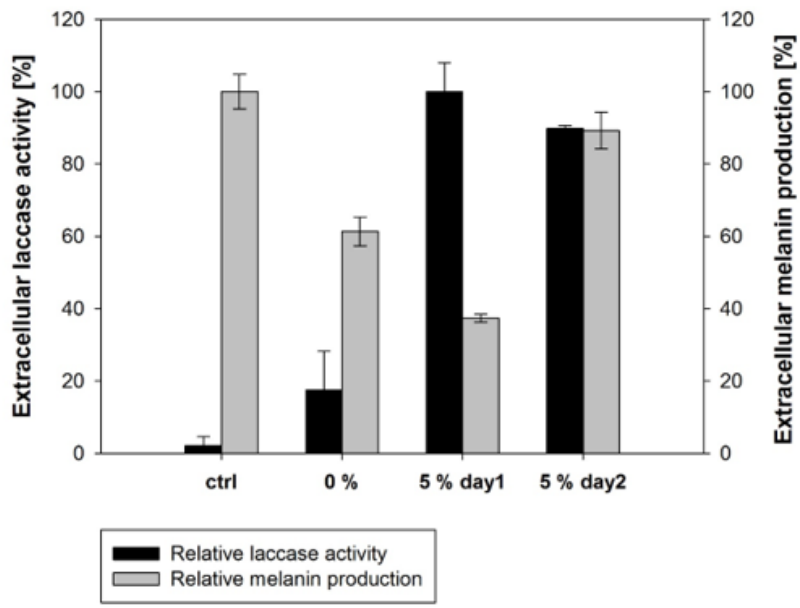

Figure 3.1. (b) Laccase activity of supernatants. The average of three different experiments with 1 standard deviation (SD) is shown.

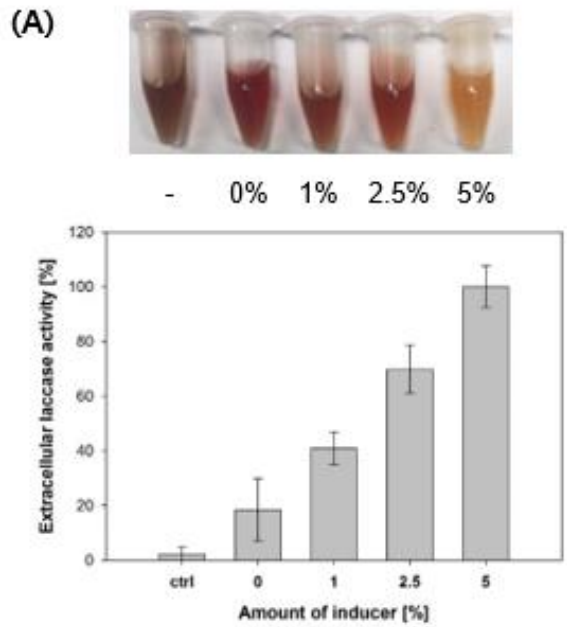

Figure 3.2. (a) The effect of induction conditions on volumetric activities of extracellular laccase. The S.glaucescens recombinant cells were grown in shake flasks at 30 ℃ and induced with DL-fructose as described in Methods. 200 μL of supernatants were prepared and tested. The recombinant cells were induced at a day after inoculation with different amount of the inducer.

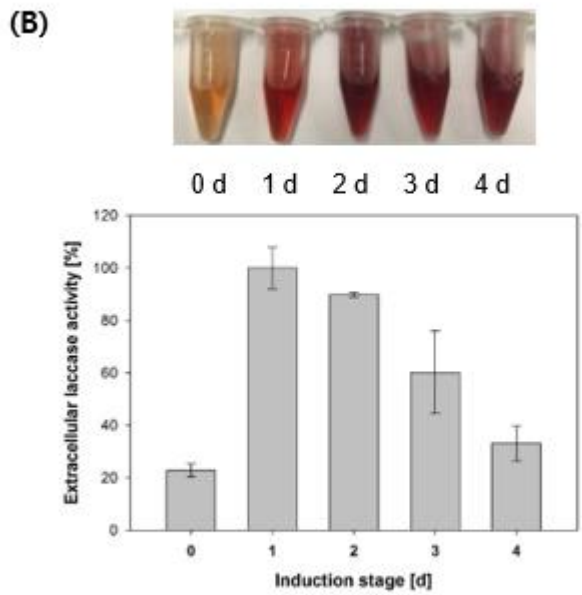

Figure 3.2. (b) The recombinant cells were induced with 5 % inducer at different stages.

(C)

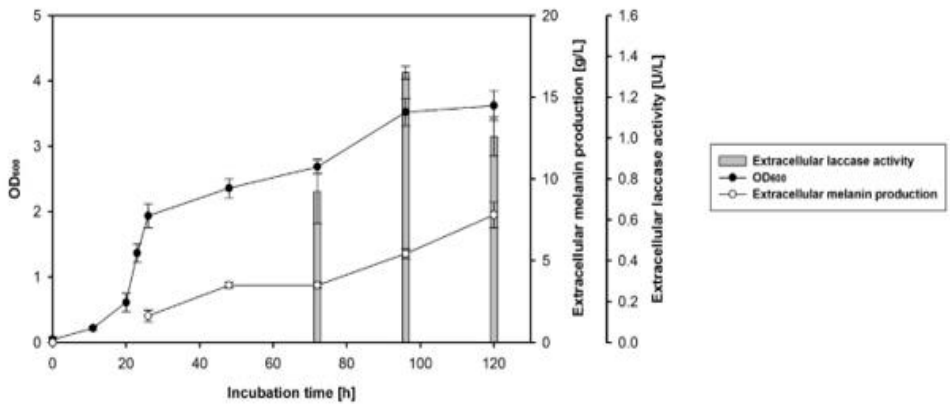

Figure 3.2. (c) The recombinant cell yy was grown was induced at 48 hr as described in Methods. Growth (●), extracellular activity (○) and extracellular melanin production(▌) were determined as indicated in Methods. Data points are the averages of the results of three measurements.

The effects of cell-soup treatment conditions on the dyeing performance were observed in terms of K/S value of the dyed samples (Fig.3.3, Table 3.1, and Table 3.2) The cell supernatant colored the wool fabrics to yellow-red or red.

However, it showed that laccase involvement in the cell soup provided the enhanced color depth. The sample, which was treated using laccase-induced cell soup in pH 5 buffer solution, indicated nearly 4.6 times higher K/S value than that of control group as well as 1.7 times in pH 8 buffer solution. This could be attributed to laccase that might act on the color fixation as an oxidative enzyme.

To further determine the influence of laccase secretion, additional studies were performed in two ways. First of all, when the well-known mordant, $FeSO_4$ solution, was supplied to the bath at the end of the dyeing process, the color of the control group turned to deeper color, which was similar to the color of laccase-treated group (Fig. 10). It suggested that the introduction of the mordant agent would be a major factor than a slight difference in the pigment amounts. Also, the cell soup showed the better coloration as the amount of laccase induction was increased (R^2= 0.9787, Fig.3.1(a)). The above results showed that laccase was increased in extracellular and accelerated the color fixation when the inducer was increased from 0 g/L to 2.5 g/L.

Table 3 showed the results of color fastness test of the dyed wool fabrics. The laccase-treated group (pH 5) showed better dyeing

fastness compared to the control group while the value was decreased at pH 8. It was aligned with an optimum pH of small laccase from *Streptomyces viridosporus*, which is reported to be around pH 4-5. Also, it can be mentioned that the melanin pigment had an affinity for wool fabric surface in acidic solution and reinforced the difference in color fastness.

3.3.3. Effect of Sv1 reaction on structures of the dye pigment and the colored wool fabrics

3.3.3.1 FTIR analysis of dyed wool fabric

Figure 3.3(d) shows IR spectra of an original wool sample and wool samples treated with cell supernatant of recombinant cell. There was a difference in the absorbance of peak observed around 3271.74 cm^{-1} between the wool fabrics treated by using cell. The peak around 3271.74 cm^{-1} was attributed to the hydroxyl and amino groups present on the surface of the wool fabrics. As the increasing number of melanin granules were grafted on the wool fabrics by the one-step method using cell, the sample showed weaker absorption peaks of the hydroxyl group, compared to the samples using cell. The absorption peaks at 1631.91 cm^{-1}, assigned to phenolic C=C and C=O, which were increased as there are lots of carbonyl groups in melanin. Moreover, the peaks of C=C and C=O in the sample treated by using cell shifted to lower wavenu

mbers, due to the formation of a conjugated structure. The absorption peaks at 1448.11 cm−1, 1390.29 cm−1, and 1233.22 cm−1 can be attri buted to the C–H asymmetric vibrations, symmetric umbrella like vibrati ons, and rocking modes, respectively. These results demonstrate that melanin was successfully grafted by using cell supernatants of recombinant cell

3.3.3.2 Surface morphology of dyed wool fabric

Morphological changes in the wool fabrics were distinguished by scanning electron microscopy (Fig.3.3(a)). The flakes or particles of melanin were deposited on the surfaces of samples. The surface of control group looked smoother than those of wool samples, which were treated with cell supernatant of recombinant cell. These results indicate that the larger amount of pigment was attached to the surface when the wool fabrics were dyed with laccase-inducing cell supernatant.

3.4. Conclusion

Prior work has provided the feasibility studies of employing purified laccases as a mordant enzyme in the coloration process. However, it still costs too much to compete against the chemical counterparts. This study aimed to devising the lower-cost method using the dyeing cell. These results provide compelling evidence for the secretory expression of

(A)

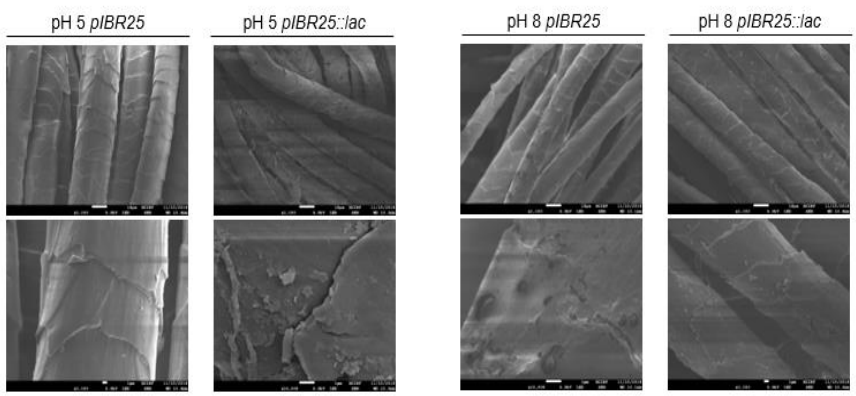

Figure 3.3. (a) SEM images of untreated wool fabric, wool fabric treated with supernatants of cell xx at pH 5/8 and wool fabric treated with supernatants of induced cell yy at pH 5/8, from left to right. Top; amplified at 1.00 k. Bottom: amplified at 3.00 k/ 10.0 k.

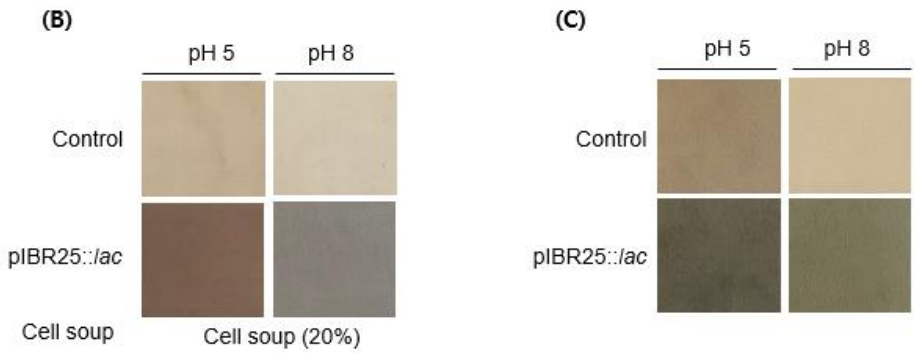

Figure 3.3. (b) Photographs of wool fabrics enzymatically dyed with supernatants at pH 5, 8 after (c) doping treatment with 2 mM $FeSO_4$ solution. The cultures were grown in R2YENG media for 120 h as described in Methods.

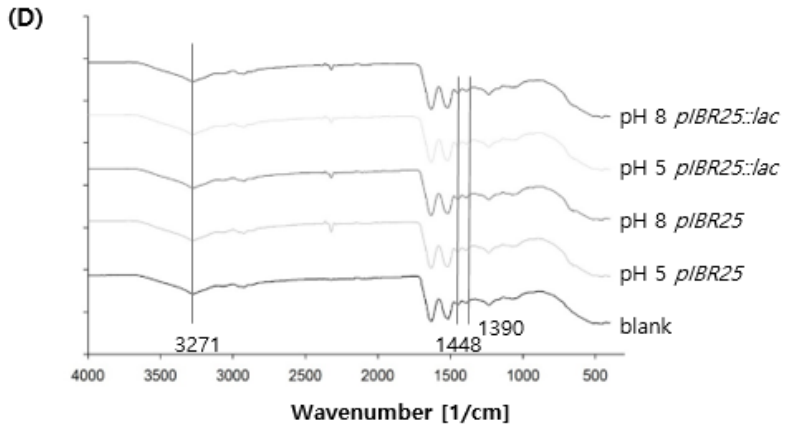

Figure 3.3. (d) FT-IR spectra of the dyed wool fabrics.

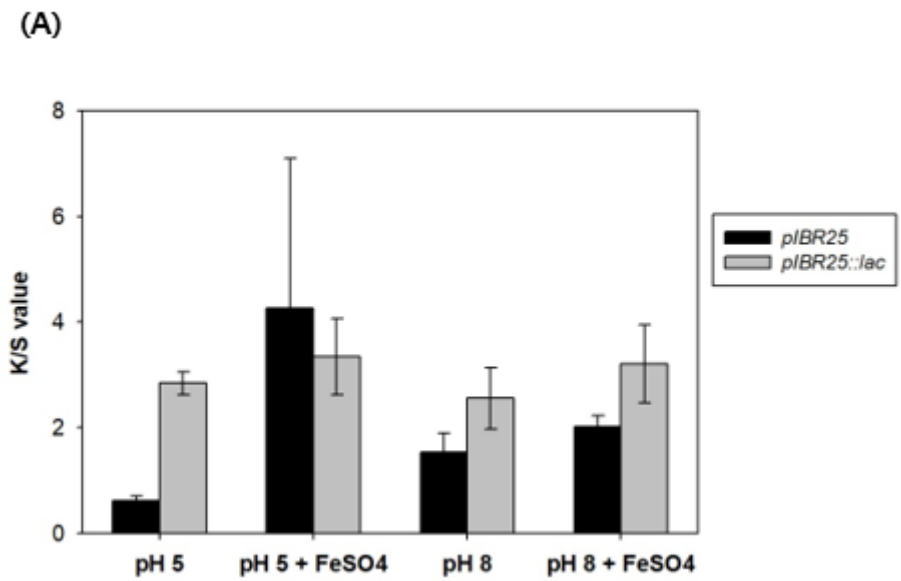

Figure 2.4 The extracellular laccase activity of grafting the natural pigment onto the wool fabric. The *S.glaucescens* recombinant cell media were prepared for dyeing the wool fabric in three different experiments. Bars represent the average K/S value of 3 trials. (a) Black bars represent the wool fabric dyed using recombinant cell xx medium(black) and grey bars represent the counterpart dyed using cell yy medium. Each sample was treated at different conditions(pH, addition of $FeSO_4$). (b)Black bars represent the average K/S value and grey bars represent the extracellular laccase activity. The recombinant cells were induced at different conditions(concentration, stage).

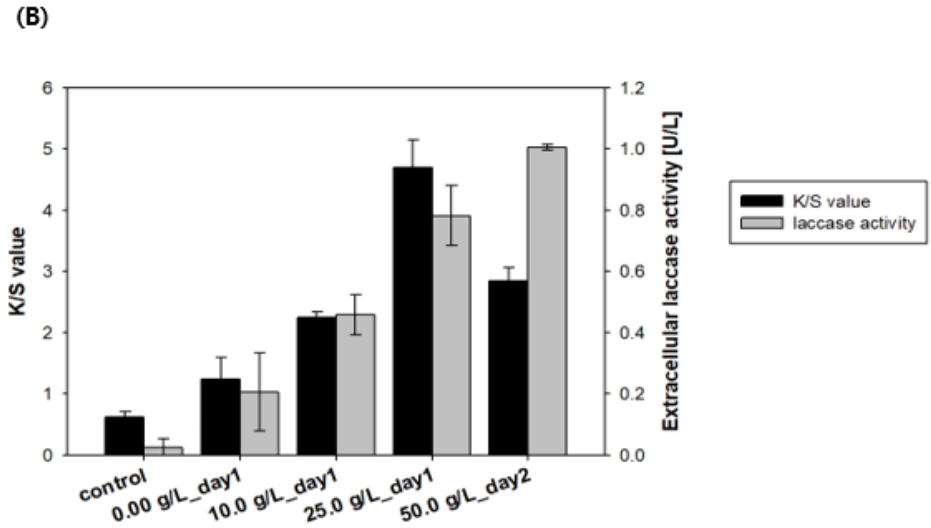

Figure 3.5 (b) Black bars represent the average K/S value and grey bars represent the extracellular laccase activity. The recombinant cells were induced at different conditions(concentration, stage).

Table 3.1. CIELAB coordinates of the colored wool fabrics

Sample	pH	K/S(530nm)	L*	a*	b*	Hue	Value	Chroma
Control	5	0.628	67.77	8.25	5.66	6.8R	6.63	2.42
Laccase-inducing	5	2.868	57.07	13.01	17.9	3.6YR	5.59	4.06
Control	8	1.657	68.33	8.99	17.53	6.2YR	6.72	3.39
Laccase-inducing	8	2.344	64.56	12.75	25.74	6.7YR	6.36	4.87

Table 3.2. Color fastness test

Sample	pH	Washing fastness		
		change in colour	staining-cotton	staining-wool
Control	5	4	4-5	4-5
Laccase-inducing	5	4-5	4-5	5
Control	8	3	4-5	5
Laccase-inducing	8	1-2	4	5

laccase and suggest that this approach appears to be effective in wool dyeing with natural microbial melanin. As laccase are being involved in diverse industries, we can also expect its application into bio-sensing electrode, water bio-remediation, and so on.

Appendix

Site-specific *o*-methylation of EGCG using Bacillus *o*-methyltransferases

S1. Introduction

Tea is one of the most commonly consumed beverage around the world. Green tea is rich in polyphenol, and tea catechins account for 60-80 % of total polyphenols. Recently, epigallocatechin 3-o-(3"-o-methyl)-gallate (EGCG3"me)-enriched tea has shown significantly improved physiological functions in animal and human model study. Several *In vivo* studies reported that EGCG3″ me exhibited better antiallergy, antiobesity, prevention of cardiovascular disease, and anticancer activity than EGCG. The stronger bioactivity of EGCG3"me seemed to be related to methyl effect which increased membrane permeability and metabolic stability. In rat's pharmacokinetic study, the bioavailability of EGCG3"me after oral administration was 1.8 and 2.7 times as much as that of EGCG4"me and EGCG, respectively.

Researchers have tried to figure out its natural occurrence by screening EGCG3″ me contents in tea cultivars. For example, EGCG3"me-enriched tea cultivars were mainly distributed in East Asia (e.g., Japan, Korea and, China). Unfortunately, EGCG3"me existed in very limited amount in natural green tea (> 1 (w/w) %), which made it very hard to extract enough amount to meet all needs. This led to obtaining EGCG3″ me in an alternative way via chemical or enzymatic reaction. Tomohiro

Asakawa et al. (2016) was able to achieve chemical synthesis of EGCG3"me but it took extra steps to introduce protecting groups onto labile polyphenols before condensation of epigallocatechin and 3"-o-methyl gallic acid. Besides, plant caffeoyl-coA o-methyltransferase could add methoxy group to EGCG without resorting to expensive multistep protection/deprotection. It also carried out o-methylation under very mild condition and without any C-methylated byproducts. Caffeoyl-coA o-methyltransferase (CCoAOMT) belongs to SAM dependent o-methyltransferase that transfers methyl group of SAM to an aromatic ring in monolignols. Similarity on the structure between caffeoyl and galloyl group enable CCoAOMT to accept EGCG as a substrate.

Some research groups have already cloned o-methyltransferases from green tea(*Camellia sinensis*) and edible mushroom (*Flammulina velutipes*) in E.coli and the results indicated that they efficiently methylated EGCG. However, it was still hard to control regioselectivity on EGCG methylation because we don't have the vaguest idea about what determines its regioselectivity. So, we focused on the methylation sites on EGCG. The possible structures of the methylated products other than EGCG3"me are epigallocatechin 3-O-(3'-O-methyl)-gallate(EGCG'me), epigallocatechin 3-O-(4'-O-methyl)-gallate(EGCG4'me), epigallocatechin 3-O-(4"-O-methyl)gallate, and multiply methylated products with similar patterns. Among them , EGCG3"me has a methyl group on 3" hydroxyl

groups of D-ring and has stronger *in vivo* bioactivity.

In this study, we found out new *Bacillus* caffeoyl-coA o-methyltransferases and expressed them in *E.coli* system. HPLC analysis and ^{1}H NMR spectrometry were applied into characterizing their activities and regioselectivities. These results will shed light on a role of each substrate binding-site residue in the regioselectivity.

S2. Material and methods

S2.1. Chemicals and materials

EGCG, S-adenosyl methionine hydrochloride (SAM·HCl) and Isopropyl-thio-β-D-galactopyranoside (IPTG) were purchased from Sigma-Aldrich (St.Louis, MO, USA). Ethyl acetate and hydrochloric acid were obtained from Junsei (Tokyo, Japan). Bacteriological agar and Luria Bertani (LB) broth were purchased from BD difco (Franklin Lakes, NJ, USA). Oligomers and sequencing were purchased from Bionics (Seoul, South Korea). Enzymes involved in restriction reaction, ligation, and PCR were purchased from Thermo Scientific, Promega, and Novagen.

S2.2. Plasmid construction

The *E.coli* DH5α strain was used for cloning. *Bacillus megaterium* Bm3, *Bacillus licheniformis* KCCM12145, and *Bacillus thuringiensis* KCCM41613 were obtained from the Korean Agricultural Culture Collection (KACC, Daejeon, South Korea). Each gene sequences were assessed from National Center for Biotechnology Information(NCBI). Bmomt, Blomt, Btomt, SAHH genes were amplified from genomic DNA using oligonucleotides by PCR thermocycler. Bmomt, Btomt, and SAHH genes were inserted into the *Nco*I and *Xho*I sites of the pET28a(+) expression vector (novagen, USA). Blomt gene was inserted into the *Nde*I and *Xho*I sites of the pET24ma (novagen, USA). All DNA manipulations for cloning were performed following standard procedures.

S2.3. Expression and purification of the enzymes

For the expression and purification of the enzymes, each of the constructed plasmid DNA were transformed into E.coli BL21 (DE3) using standard heat shock method and each colony of the transformants from agar plate was cultured in 2mL of LB medium containing appropriate antibiotics at 37 ℃ overnight. Then, the precultured cells were inoculated

and cultured into 50 mL of LB medium until the $O.D._{600}$ reached around 0.6-0.8. IPTG was added to the culture to a final concentration of 0.1 mM, and the cells were cultured at 18 ° C for 18 hrs with shaking. The cultures were then centrifuged to harvest the cells, which were then washed with 100 mM phosphate buffer (pH 7.4) and resuspended in lysis buffer (50 mM NaH_2PO_4, 300 mM NaCl, 5 mM imidazole, pH 8.0). The cell suspension was then sonicated and centrifuged again, and the supernatant was used for purification. Bm-OMT, Bl-OMT, Bt-OMT, and SAH nucleosidase were purified using a His-tag column (QIAGEN Kora Ltd., Seoul, South Korea) washed with wash buffer(50 mM NaH_2PO_4, 300 mM NaCl, 20 mM imidazole, pH 8.0), and then eluted with 50 mM sodium buffer (pH 7.4) containing 250 mM imidazole. For proper storage of the enzymes, NaCl and imidazole were removed and the final eluted fractions were concentrated by ultrafiltration dialysis. The enzyme expression and purification were confirmed by sodium dodecyl sulfate polyacrylamide gel electrophoresis (SDS-PAGE) analysis and the amound of each enzyme in the samples was measured using Bradford protein assay.

S2.4. Determination of enzyme activity

The purified enzymes were used to verify their catalytic activities. To evaluate whether methyl groups were attached into phenoxyl groups of

EGCG, 10 μM of o-methyltransferase and 2 μM of SAH nucleosidase were introduced into 0.2 mL reaction system containing 0.5 mM EGCG, 1 mM SAM, 0.2 mM MgCl2, 10 mM ascorbic acid, and 100 mM tris-HCl buffer (pH 7.5). The reaction mixture was incubated at 30 ℃ for 5 hrs and the reaction was stopped by addition of 1 N HCl. Then, the mixture was extracted with 0.8 mL of ethyl acetate, and the organic phase was evaporated to dryness. Finally, the residue was resuspended in methanol.

All the product concentrations were experimentally measured for determining the kinetic parameters. The resuspended products were analyzed using a Younglin high-performance liquid chromatography (HPLC) equipped with a UV detector or Ms. A Waters C18 column (150 mm× internal diameter, 5 μm particle size) was selected as the stationary phase, and the column temperature was set at 30 ℃. The binary solution was 1 % formic acid solution (A) and acetonitrile containing 1 % formic acid (B). The gradient elution started with 15 % solvent B for 5 min, increased linearly to 27 % solvent B over 15 min, and continued to increase to 40 % solvent B over 3 min before decreasing to 15 % solvent B over 2 min and holding the same condition for 3 min. The flow rate was 0.4 mL/min and the injected volume was 10 μL. The mass accuracy was controlled through online calibration using reference ions (*m*/*z* 121.0509, 922.0098). The capillary voltage, temperature, nebuliser pressure, and flow rate of the drying gas were set to 3.5 kV, 300 ° C, 35 psi (1 psi=6.895 kPa), and 8 L/min, respectively. Mass spectra were

recorded for the *m*/*z* range of 100–1000. For accurate identification, the methylated products were subjected to the accurate mass, mass patterns, and retention time comparison with authentic standards.

S2.5. Purification and NMR spectroscopy of *o*-methylated EGCGs

The isolation and purification of compounds were performed with a Younglin HPLC system, L-7150 pump, L-7420 UV–vis detector, and D-2500 Chromato-Integrator (Hitachi, Ltd., Japan). The reaction mixture was scaled up to 10 mL, but the reaction condition was the same as described before. The mixture was incubated at 30 ° C for 18 h and extracted with ethyl acetate. Removal of ethyl acetate by evaporation gave a solid mixture of *o*-methylated EGCGs. The *o*-Methylated EGCGs were fractionated by HPLC with the reversed-phase column Inertsil ODS-3 (20 mM i.d. × 250 mM, GL Sciences Inc., Japan). The detection wavelength was 280 nm, flow rate was 0.6 mL/min, and mobile phase was 0.1 % TFA solution (A)/CAN containing 0.1% TFA. The gradient elution started with 15 % solvent B for 5 min, increased linearly to 27 % solvent B over 15 min, and continued to increase to 40 % solvent B over 3 min before decreasing to 15 % solvent B over 2 min and holding the same condition for 3 min. Each fraction was extracted with ethyl acetate. After evaporation, 11.92 and 0.92 mg of compounds 1 and 2, respectively, were

obtained as white amorphous powders. ^{1}H NMR (600 MHz) spectra were recorded according to a previously described method using the Bruker AV600 instrument (Bruker BioSpin GmbH, Germany).

S3. Results and discussion

S3.1. Expression and purification of recombinant o-methltransferases from *Bacillus* in *E.coli* system

Phylogenetic analysis of o-methyltransferase sequences provided that BlOMT, and BtOMT belonged to the two different clusters. The protein sequence alignment showed that BmOMT, BlOMT, and BtOMT showed 48 - 56 % of high similarity with other OMTS from *Bacillus cereus* and *Streptomyces avermitilis*, and also displayed 30 - 40 % of similarity with CCoAOMTs from plants. All the three Bacillus o-methyltransferases had the highly conserved SAM binding residues, some of which are conserved in class I o-methyltransferase; residue Ser 73, Glu 91, Asp 141, and Asp 143, possible H-bond donors or acceptors were conserved.

While several plant or bacterial OMTs have shown the possible involvement of the relatively varied sequence either at N-terminal or C-terminal region in the substrate specificity, these three Bacillus OMTs

lacked the extended N-terminal residues commonly found in other plant OMTS. Therefore, the substrate specificity might depend on the distinct insertion loop between β5 and α9, constituting a part of substrate binding pocket at C-terminal. It was reported that the loop changed the pocket shape upon SAH binding, and determined the substrate specificity in other OMTs.

BmOMT, Blomt, and Btomt were successfully expressed in soluble fraction of *E.coli* strain Bl21(DE3), supported by SDS-PAGE gel analysis (Fig.S1). Each of the his-tag purified enzymes was used for further functional characterization.

S3.2. Enzyme activity and regiospecificity on EGCG

To understand enzyme performance, we did HPLC analysis of in vitro reactions with BmOMT, BlOMT, and BtOMT. BmOMT and BlOMT generated new product peaks whereas BtOMT could not (Fig.S2). We also quantified the substrate conversion to evaluate the kinetic parameters toward SAM. In reactions of OMTS with the methyl donor SAM at concentrations ranging from 50 to 250 μmol/L, Bmomt and Blomt catalyzed the formation of methylated EGCG with an apparent K_m value

of 17.67, 589.28 μmol/L and an apparent K_{cat} value of 6.59, 3.00 s^{-1}. At the every condition, BmOMT exhibited higher activity than BlOMT.

Next, we identified the product peaks and examined the position of the methoxy group in the o-methylated EGCG products. Figure 13 showed the HPLC profile over time in the reaction mixture of BmOMT and BlOMT. There were several o-methylated products, among which the four product peaks (1,2,3,4,5) were eluted at 7.3, 12.2, 12.6, 17.6, 20.7 min. The MS/MS patterns and ^{1}H NMR spectra (Fig. S3) indicated that the products were identified as epigallocatechin 3-o-gallate (compound 1, EGCG), epigallocatechin 3-o-(4"-o-methyl)-gallate (compound 2, EGCG4"me), epigallocatechin 3-o-(3"-o-methyl)-gallate (compound 3, EGCG3"me), epigallocatechin 3-o-(3",5"-o-dimethyl)-gallate (compound 4, EGCG3"5"dime), epigallocatechin 3-o-(3",4"-o-dimethyl)-gallate (compound 5, EGCG3"4"dime).

Taken together, BmOMT and BlOMT only transferred a methyl group to 3" or 4" hydroxyl group of EGCG. Interestingly, BmOMT preferred to produce 3"-o-methylated product (B) over 4"-o-methylated products (A). The ratio of 3"-o-methylated EGCG to 4"-o-methylated EGCG was around 8.4. Likewise, BmOMT produced 3", 5"-o-dimethylated EGCG much more than 3", 4"-o-dimethylated EGCG, a ratio of which

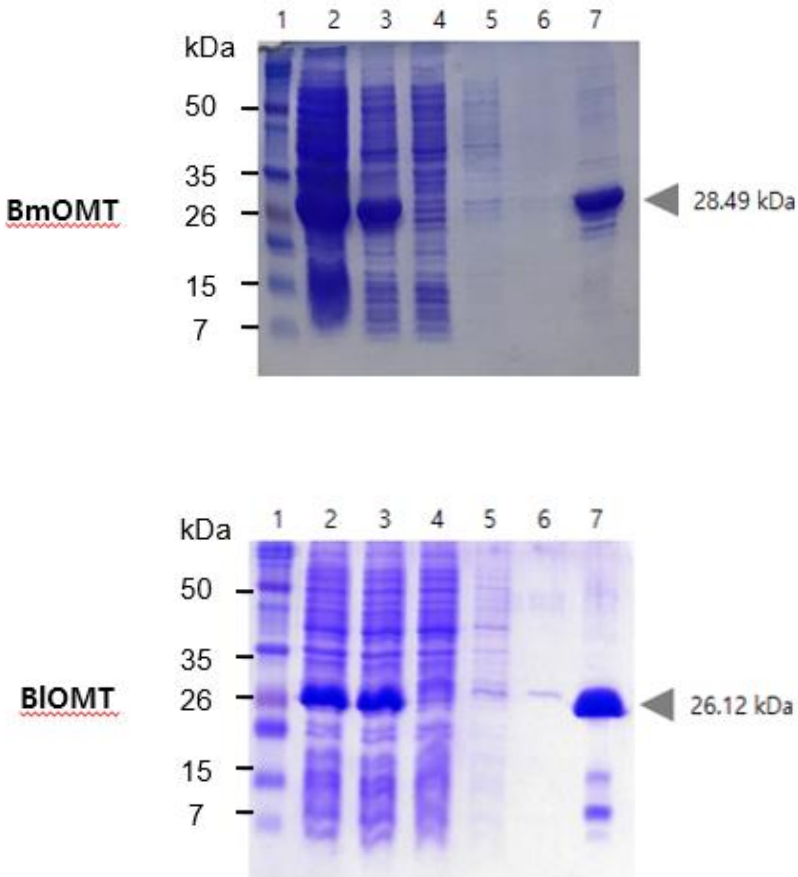

Figure S1. Analysis of OMT and SAH hydrolase expression and purification. 1, marker; 2, total protein induced with IPTG for 18 h; 3, soluble protein in the supernatant induced with IPTG for 16 h; 4, soluble protein unbound in the his-tag affinity column; 5,6, the column flow-through of other bacterial enzymes contaminating the supernatant; 7, soluble protein purified in mM imidazole solution.

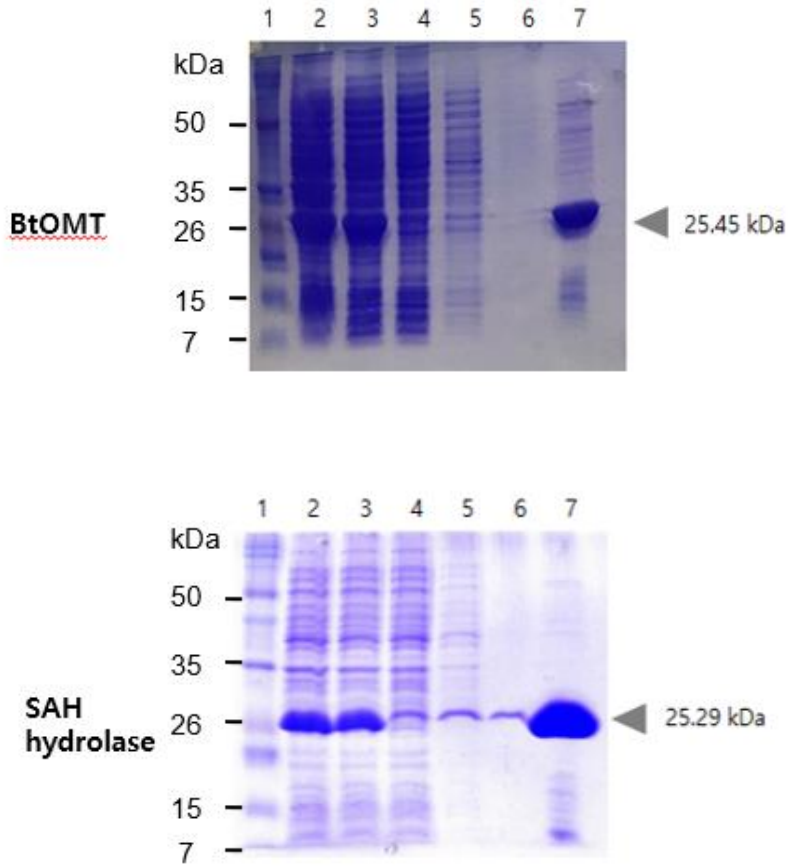

Figure S1. Analysis of OMT and SAH hydrolase expression and purification. 1, marker; 2, total protein induced with IPTG for 18 h; 3, soluble protein in the supernatant induced with IPTG for 16 h; 4, soluble protein unbound in the his-tag affinity column; 5,6, the column flow-through of other bacterial enzymes contaminating the supernatant; 7, soluble protein purified in mM imidazole solution.

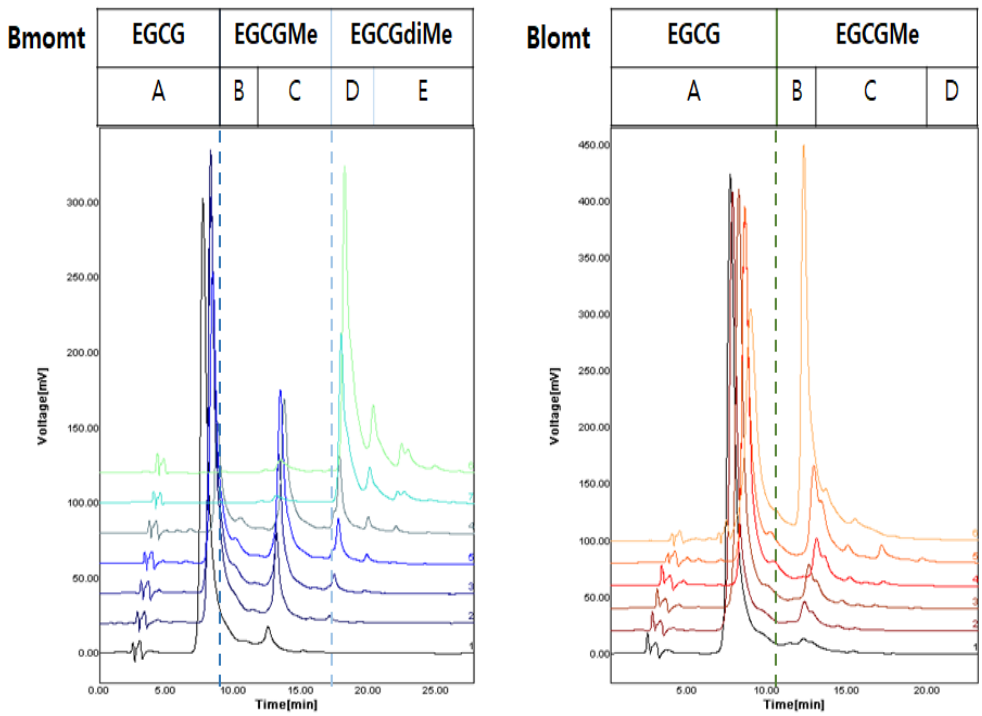

Figure S2. HPLC analysis of enzymatic reaction products using recombinant BmOMT and BlOMT enzyme. UV-vis spectra showed time-dependent changes in reaction catalyzed by BmOMT and BlOMT.

was around 6.8, as it recognized the mono-methylated EGCG as a substrate and formed dimethylated EGCG products.

Taken together, BmOMT and BlOMT only transferred a methyl group to 3" or 4" hydroxyl group of EGCG. Interestingly, BmOMT preferred to produce 3"-o-methylated product (B) over 4"-o-methylated products (A). The ratio of 3"-o-methylated EGCG to 4"-o-methylated EGCG was around 8.4. Likewise, BmOMT produced 3", 5"-o-dimethylated EGCG much more than 3", 4"-o-dimethylated EGCG, a ratio of which was around 6.8, as it recognized the mono-methylated EGCG as a substrate and formed dimethylated EGCG products.

S3.3. Optimization of EGCG 3"me production

All reactions were carried out with antioxidant ascorbic acid under moderate temperature 30 ℃ because labile EGCG and its methylated analogs require very careful control to prevent auto-oxidation. Other than that, we presumed that EGCG3"me production are related to pH and SAM concentration and optimized the reaction conditions.

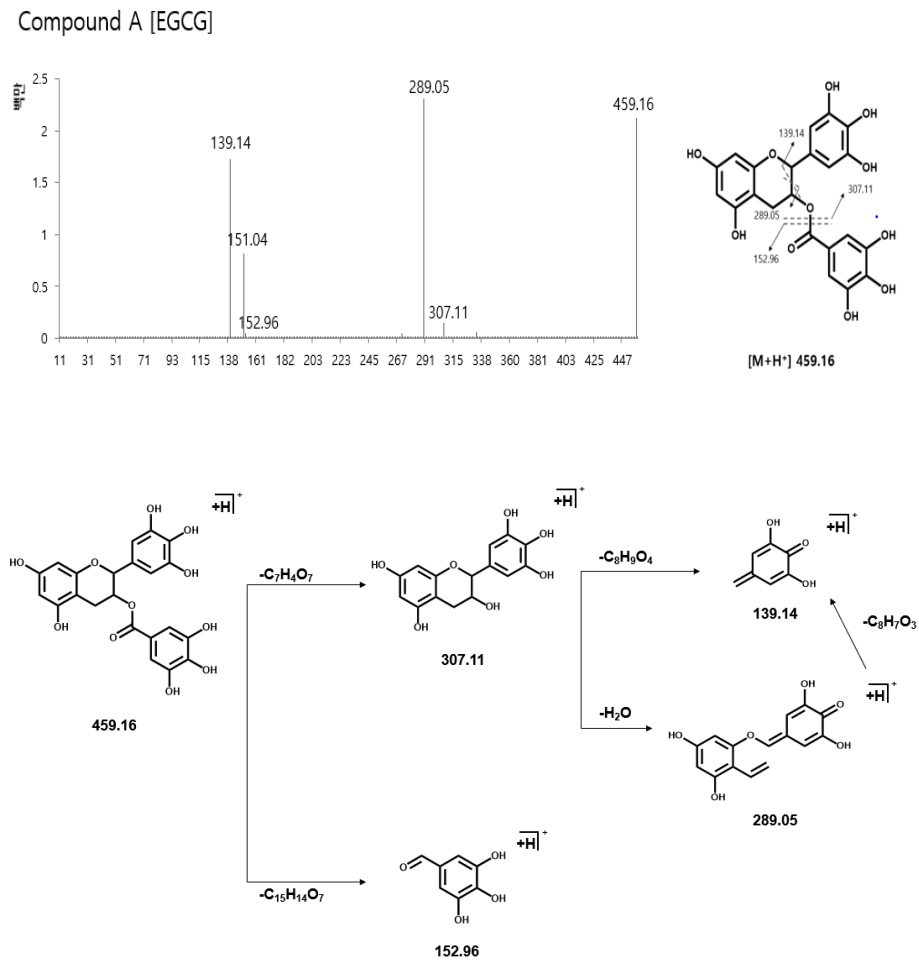

Figure S3. ESI-MS/MS patterns for compounds A, C, and D

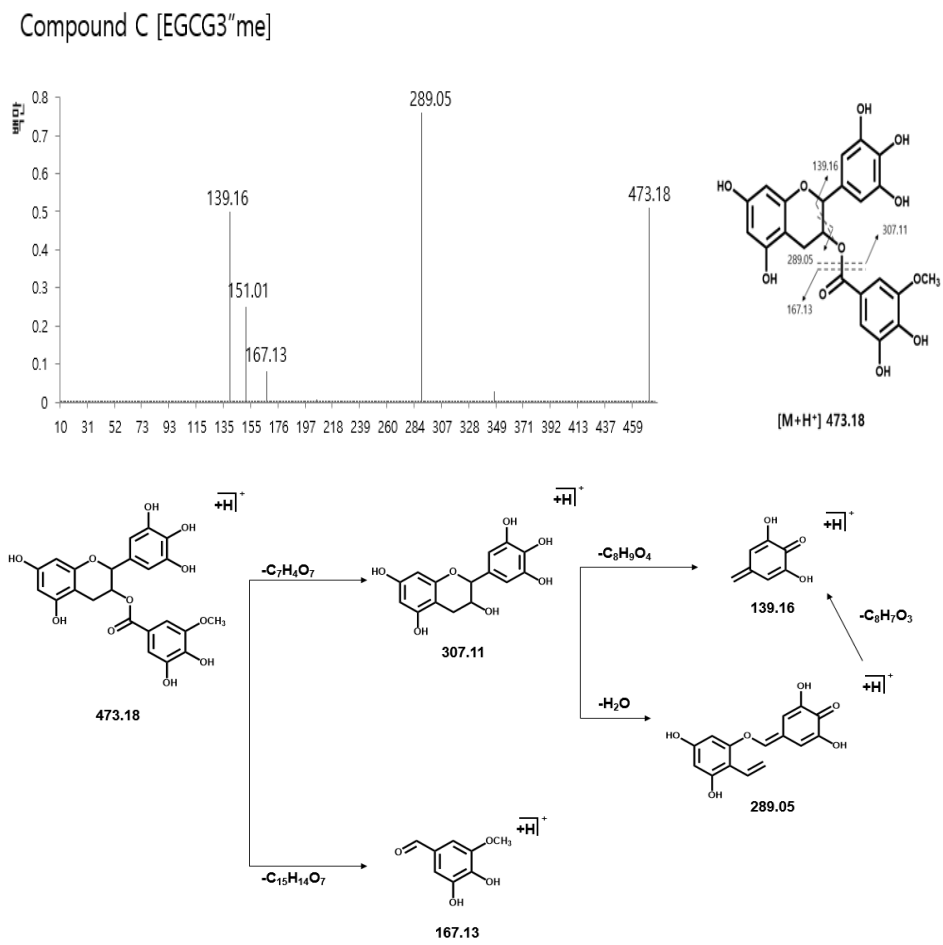

Figure S3. ESI-MS/MS patterns for compounds A, C, and D

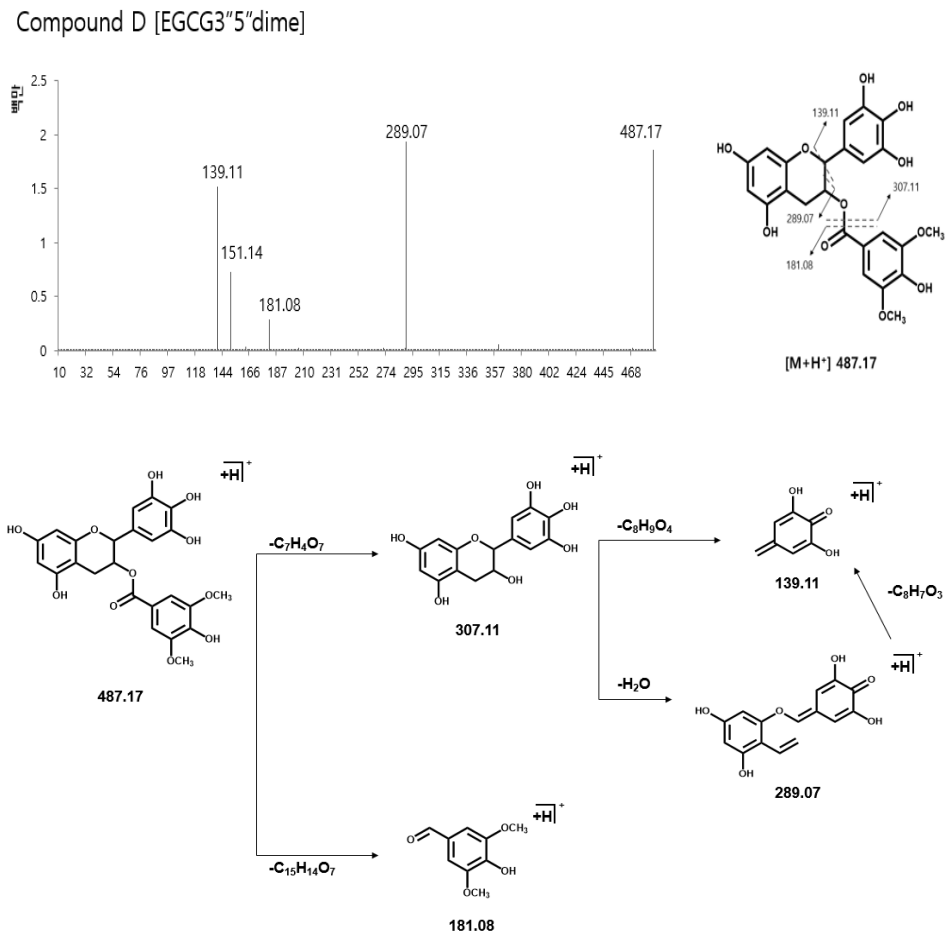

Figure S3. ESI-MS/MS patterns for compounds A, C, and D

Table S1. Assignment of ^{1}H NMR data of compounds C and D from EGCG produced by BmOMT

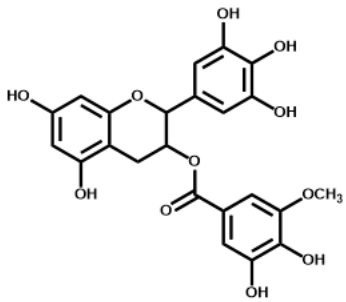

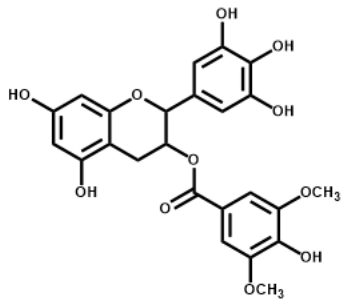

Position	Compound C	Compound D
2	4.99 (s)	5.03 (s)
3	5.31 (m)	5.39 (m)
4a	2.92 (m)	2.95 (m)
4b	2.71 (m)	2.72 (m)
6	5.93 (d)	5.83 (d)
8	5.83 (d)	5.92 (d)
2′/6′	6.41 (s)	6.43 (s)
2″	6.94 (d)	7.20 (s)
6″	6.88 (d)	7.20 (s)
OCH_3	3.73 (s)	3.74 (s)

BmOMT and BlOMT were stable for 18 hours in pH around 7.0-8.5, and they had the greatest activity at pH 7.5 and 8.0, respectively. Also, SAM as the methyl donor played an important role in changing the number and type of the products. For BmOMT, the EGCG derivatives with multiple methyl groups became dominant with increasing concentration of SAM. When molar ratio of SAM to EGCG was over 2, the number of methyl transfer to EGCG exceeded that to EGCG3"me, and therefore EGCG3"me production decreased. In contrast, EGCG3" me production from BlOMT increased proportionally to the amount of SAM.

S4. Conclusion

In this study, EGCG3"me was produced using through methyl transfer reaction from *Bacillus* o-methyltransferases. We first found out new bacterial o-methyltransferases that have excellent activity toward EGCG and successfully expressed them in *E.coli* system. Electrospray ionization tandem LC-MS (ESI-LC/MS) and ^{1}H NMR were used to determine the methylated products, EGCG3"me, EGCG4"me, EGCG3"5"dime, and EGCG3"4"dime. These findings will guide generation of invaluable methylated catechins and the pharmakinetic and pharmacodynamics optimization of bioactive scaffolds for drug development.

4. References

1. Solomon EI, Augustine AJ, Yoon J (2008) O2 Reduction to H2O by the multicopper oxidases. Dalton Trans. (30): 3921. .
2. Xu F (1996), Oxidation of Phenols, Anilines, and Benzenethiols by Fungal Laccases: Correlation between Activity and Redox Potentials as Well as Halide Inhibition. Biochemistry 35 (23): 7608–7614.
3. Baldrian P (2006), Fungal laccases - occurrence and properties. FEMS Microbiol. Rev. 30 (2): 215–242.
4. Kellner H, Luis P, Zimdars B, Kiesel B, Buscot F (2008) Diversity of bacterial laccase-like multicopper oxidase genes in forest and grassland Cambisol soil samples. Soil Biol. Biochem.
5. Ausec L, Zakrzewski M, Goesmann A, Schlüter A, Mandic-Mulec I, et al. (2011) Bioinformatic Analysis Reveals High Diversity of Bacterial Genes for Laccase-Like Enzymes. PLoS ONE 6 (10): e25724.
6. Sirim D, Wagner F, Wang L, Schmid RD, Pleiss J (2011) The Laccase Engineering Database: a classification and analysis system for laccases and related multicopper oxidases. Database (Oxford) 2011: bar006.
7. Hullo MF, Moszer I, Danchin A, Martin-Verstraete I (2001) CotA of Bacillus subtilis is a copper-dependent laccase. J. Bacteriol. 183 (18): 5426–5430.
8. Outten FW, Huffman DL, Hale JA, O'Halloran TV (2001) The

independent cue and cus systems confer copper tolerance during aerobic and anaerobic growth in Escherichia coli. J. Biol. Chem. 276 (33): 30670–30677.

9. Grass G, Rensing C (2001) CueO is a multi-copper oxidase that confers copper tolerance in Escherichia coli. Biochem. Biophys. Res. Commun. 286 (5): 902–908.

10. Schelder S, Zaade D, Litsanov B, Bott M, Brocker M (2011) The two-component signal transduction system CopRS of Corynebacterium glutamicum is required for adaptation to copper-excess stress. PLoS ONE 6 (7): e22143.

11. Miyazaki K (2005) A hyperthermophilic laccase from *Thermus thermophilus* HB27. Extremophiles 9 (6): 415–425.

12. Ruijssenaars HJ, Hartmans S (2004) A cloned *Bacillus halodurans* multicopper oxidase exhibiting alkaline laccase activity. Appl. Microbiol. Biotechnol. 65 (2): 177–182.

13. Machczynski MC, Vijgenboom E, Samyn B, Canters GW (2004) Characterization of SLAC: a small laccase from *Streptomyces coelicolor* with unprecedented activity. Protein Sci. 13 (9): 2388–2397.

14. Hakulinen N, Kiiskinen L, Kruus K, Saloheimo M, Paananen A, et al. (2002) Crystal structure of a laccase from *Melanocarpus albomyces* with an intact trinuclear copper site. Nat. Struct. Biol. 9 (8): 601–605.

15. Endo K, Hayashi Y, Hibi T, Hosono K, Beppu T, et al.

(2003) Enzymological characterization of EpoA, a laccase-like phenol oxidase produced by *Streptomyces griseus.* J. Biochem. 133 (5): 671–677.

16. Endo K, Hosono K, Beppu T, Ueda K (2002) A novel extracytoplasmic phenol oxidase of *Streptomyces*: its possible involvement in the onset of morphogenesis. Microbiology (Reading, Engl.) 148 (Pt 6): 1767–1776.

17. H. Gang, D. Lee, K.-Y. Choi, H.-N. Kim, H. Ryu, D.-S. Lee and B.-G. Kim, *ACS Sustainable Chemistry & Engineering*, 2017, **5**, 4582-4588.

18. J. O. Akindoyo, M. Beg, S. Ghazali, M. Islam, N. Jeyaratnam and A. Yuvaraj, *Rsc Advances*, 2016, **6**, 114453-114482.

19. O. Bayer, W. Siefken, H. Rinke, L. Orthner and H. Schild, *German Patent DRP*, 1937, **728981**.

20. R. Perlack, L. Wright, A. Turhollow, R. Graham, B. Stokes and D. Erbach, *Washington, DC: US Department of Energy*, 2005.

21. B. Nohra, L. Candy, J.-F. Blanco, C. Guerin, Y. Raoul and Z. Mouloungui, *Macromolecules*, 2013, **46**, 3771-3792.

22. I. Javni, W. Zhang and Z. S. Petrović, *Journal of Applied Polymer Science*, 2003, **88**, 2912-2916.

23. B.-L. Xue, J.-L. Wen and R.-C. Sun, *ACS Sustainable Chemistry & Engineering*, 2014, **2**, 1474-1480.

24. C. Zhang, R. Ding and M. R. Kessler, *Macromolecular rapid communications*, 2014, **35**, 1068-1074.

25. B. M. Upton and A. M. Kasko, *Chemical reviews*, 2016, **116**, 2275-2306.

26. G. A. Phalak, D. M. Patil and S. Mhaske, *European Polymer Journal*, 2017, **88**, 93-108.

27. J.-Y. Liang, S.-R. Shin, S.-H. Lee and D.-S. Lee, *Polymers*, 2019, **11**, 1674.

28. K. Sheeja and A. T. Booshan, *Inter. J. Develop Res*, 2014, **4**, 2246-2252.

29. J. Wan, B. Gan, C. Li, J. Molina-Aldareguia, E. N. Kalali, X. Wang and D.-Y. Wang, *Chemical Engineering Journal*, 2016, **284**, 1080-1093.

30. K. Sakai, H. Takeuti, S.-P. Mun and H. Imamura, *Journal of wood chemistry and technology*, 1988, **8**, 29-41.

15. G. P. Kamatou, I. Vermaak and A. M. Viljoen, *Molecules*, 2012, **17**, 6953-6981.

31. D. C. Dayton, J. R. Carpenter, A. Kataria, J. E. Peters, D. Barbee, O. D. Mante and R. Gupta, *Green Chemistry*, 2015, **17**, 4680-4689.

32. W. Schutyser, T. Renders, S. Van den Bosch, S.-F. Koelewijn, G. Beckham and B. F. Sels, *Chemical Society Reviews*, 2018, **47**, 852-908.

33. K. P. Devi, S. A. Nisha, R. Sakthivel and S. K. Pandian, *Journal of ethnopharmacology*, 2010, **130**, 107-115.

34. S. Krist, L. Halwachs, G. Sallaberger and G. Buchbauer, *Flavour and fragrance journal*, 2007, **22**, 44-48.

35. V. Navikaite-Snipaitiene, L. Ivanauskas, V. Jakstas, N. Rüegg, R. Rutkaite, E. Wolfram and S. Yildirim, *Meat science*, 2018, **145**, 9-15.

36. C. Li, Y. Chen, X. Cai, G. Yang and X. S. Sun, *ACS Sustainable Chemistry & Engineering*, 2020, **8**, 3553-3560.

37. C. Cheng, X. Zhang, X. Chen, J. Li, Q. Huang, Z. Hu and Y. Tu, *Journal of Polymer Research*, 2016, **23**, 110.

38. C. Cheng, J. Li, F. Yang, Y. Li, Z. Hu and J. Wang, *Journal of Polymer Research*, 2018, **25**, 57.

39. M. Kessler, *Proceedings of the Institution of Mechanical Engineers, Part G: Journal of Aerospace Engineering*, 2007, **221**, 479-495.

40. N. K. Guimard, K. K. Oehlenschlaeger, J. Zhou, S. Hilf, F. G. Schmidt and C. Barner-Kowollik, *Macromolecular Chemistry and Physics*, 2012, **213**, 131-143.

41. X. Huang, C. Craita, L. Awad and P. Vogel, *Chemical communications*, 2005, 1297-1299.

42. Luqman Jameel Rather, Shahid-ul-Islam, Mohd Shabbir, Mohd Nadeem Bukhari, Mohd Shahid, Mohd Ali Khan, Faqeer Mohammad. (2016), Ecological dyeing of Woolen yarn with Adhatoda vasica natural dye in the presence of biomordants as an alternative copartner to metal mordants. *Journal of Environmental Chemical Engineering*. 4.3: 3041-3049. doi:10.1016/j.jece.2016.06.019..

43. Goyer, Robert A., and Thomas W. Clarkson. (1996), Toxic effects

of metals.“ *Casarett & Doull’ s Toxicology. The Basic Science of Poisons, Fifth Edition, Klaassen, CD [Ed]. McGraw-Hill Health Professions Division*.

44. Padma S. Vankar, Rakhi Shanker, Jyoti Srivastava. (2007), Ultrasonic dyeing of cotton fabric with aqueous extract of Eclipta alba, *Dyes and Pigments*. 72.1: 33-37. doi:10.1016/j.dyepig.2005.07.013.

45. Padma S. Vankar, Rakhi Shanker, Jyoti Srivastava. (2007), Ultrasonic dyeing of cotton fabric with aqueous extract of Eclipta alba, *Dyes and Pigments*. 72.1: 33-37. doi:10.1016/j.dyepig.2005.07.013.

46. M.Rita De Giorgi, Enzo Cadoni, Debora Maricca, Alessandra Piras. (2000) Dyeing polyester fibres with disperse dyes in supercritical CO2. *Dyes and Pigments.* 45.1: 75-79. doi:10.1016/S0143-7208(00)00011-5.

47. Shahid-ul-Islam and Gang Sun. (2017) Thermodynamics, Kinetics, and Multifunctional Finishing of Textile Materials with Colorants Extracted from Natural Renewable Sources. *ACS Sustainable Chemistry & Engineering*. *5*.9: 7451-7466. doi: 10.1021/acssuschemeng.7b01486.

48. Jeon, J. , Kim, E. , Murugesan, K. , Park, H. , Kim, Y. , Kwon, J. , Kim, W. , Lee, J. and Chang, Y. (2010), Laccase-catalysed

polymeric dye synthesis from plant-derived phenols for potential application in hair dyeing: Enzymatic colourations driven by homo- or hetero-polymer synthesis. *Microbial Biotechnology.* 3: 324–335. doi:10.1111/j.1751-7915.2009.00153.x

49. Sevillano, Laura, Vijgenboom Erik & Wezel, Gilles & Díaz, Margarita & Santamaria, Ramon. (2016), New approaches to achieve high level enzyme production in Streptomyces lividans. *Microbial Cell Factories*. 15. doi:10.1186/s12934-016-0425-7.

50. Majumdar, Sudipta and Lukk, Tiit and Solbiati, Jose O. and Bauer, Stefan and Nair, Satish K. and Cronan, John E. and Gerlt, John A. (2014), Roles of small laccases in Streptoymces in lignin degradation. *Biochemistry*. *53*. 24. 4047-4058. doi:10.1021/bi500285t

51. Shin Hoonsik, Georg Guebitz, and Artur Cavaco-Paulo. (2001) "In Situ" Enzymatically Prepared Polymers for Wool Coloration. *Macromolecular Materials & Engineering* 286.11 691-694.

국문 초록

락케이즈는 미생물에서부터 고등생물까지 광범위하게 발견되고 라디칼 산화환 반응을 촉매한다. 라케이즈는 목질계 리그닌 바이오매스로부터 다양한 페놀류 단량체의 생합성에 중요한 역할을 하는 엔자임이다. 그러나, 많은 연구에서 버섯 유래 락케이즈의 최적 pH가 산성이어서 실질적인 적용이 어렵다고 보고되어 있다. 본 연구논문은 *Streptomyces viridosporus* 유래의 락케이즈 Sv1을 대장균 및 방선균에서 발현하여 신규 물질의 생합성 및 염색 균주의 개발에 적용하였다. 대장균에서 발현된 Sv1 효소는 다양한 유기용매에서 뛰어난 안정성을 보였고, 넓은 pH 범위에서 높은 활성을 보여주었다. 이를 바탕으로, 친환경적이고 효율적인 염색 미생물 균주를 개발하기 위해 R2YE 복합 배지에서 멜라닌을 다량 분비하는 *S.glaucescens* 균주에 외래 Sv1 유전자를 도입한 균주를 제작하였다. 적외선분광법과 전자 현미경 분석법을 통해 Sv1이 염료를 양모에 공유 결합으로 염착시킴을 확인할 수 있었다. 결과적으로 이러한 염색 균주를 사용하여 색차를 5 배 증진 시키고 색상 견뢰도를 한 단계 향상시킬 수 있었다. 락케이즈의 다른 사용예로서는, 자가치유 가능 폴리우레탄의 사슬 연장제로 사용 가능한 Dieugenol-based hexaol의 합성 과정 중간체인 에폭시 유지놀 이량체를 sv1을 이용하여 합성하였다. Sv1은 에폭시 유지놀의 82 % 을 이량체화 시킬 수 있었다. 그러나, 에폭사이드의 고리열림반응 효율이 낮아서 이후로는 화학적인 변형을 통해 Dieugenol-based hexaol을 합성하였고 핵자기공명분석법과 기체 크로마토그래피 질량 분석법을 통해 생성됨을 확인하였다. Dieugenol-based hexaol을 도입한 폴리우레탄은 84.7 %의 우수한 자가치유특성을 띰을 확

인할 수 있었다.

주요어: 락케이즈, Svl, 열 안정성, pH, 자가치유성, 폴리우레탄 ,염색균주

학번: 2018-27445